Electronic Supplementary Material (ESI) for ChemComm.


# Supporting Information

# Phosphorus Derivatives of Mesoionic Carbenes: Synthesis and Characterization of Triazaphosphole-5-ylidene→$BF_3$ Adducts

Lea Dettling,[a] Niklas Limberg,[a] Raphaela Küppers,[a] Daniel Frost,[a] Manuela Weber,[a] Nathan T. Coles,[b] Diego M. Andrada,[c] Christian Müller*[a]

**Table of Contents**

# 1. Experimental Procedures

## 1.1 General Information

All reactions involving air- and moisture-sensitive compounds were carried out using an *MBRAUN* glovebox under an argon atmosphere or standard Schlenk techniques. All common chemicals and solvents were commercially available. Benzylazide[1], 2-azido-1,3-diisopropylbenzene[2] and trimethylsilyl-phosphaalkine[3] were prepared by methods described in the literature. Commercially available chemicals were used without further purification. Toluene, DCM and *n*-pentane were prepared using an *MBRAUN* Solvent Purification System *MB-SPS 800*. THF and DME were dried over K/benzophenone under argon. The deuterated dry solvents DCM-$d_2$ and acetonitrile-$d_3$ were dried over $CaH_2$ and THF-$d_8$ over a sodium-potassium alloy and chloroform-*d* over molecular sieve 4Å. $^{1}H$, $^{13}C\{^{1}H\}$, $^{19}F$, $^{19}F\{^{31}P\}$, $^{11}B\{^{19}F\}$,$^{11}B$ and $^{31}P\{^{1}H\}$ NMR spectra were recorded by using a *JEOL ECS400* spectrometer (400 MHz), or a *JEOL ECZ600* spectrometer (600 MHz). All chemical shifts are reported relative to the residual resonance in the deuterated solvents.

**Caution**: Azides are potentially hazardous compounds and adequate safety measures should be taken when weighing, heating and working up.

## 1.2 Synthesis and Characterization

### 3-benzyl-5-(trimethylsilyl)-3*H*-1,2,3,4-triazaphosphole (1a)

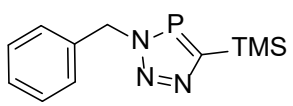


Benzylazide (200 mg, 1.50 mmol, 1.00 eq) was added to an excess of trimethylsilyl-phosphaalkine in toluene. After stirring the reaction mixture overnight at room temperature, the excess of trimethylsilyl-phosphaalkine in toluene was condensed out of the reaction mixture in a separate Schlenk flask (after determination of the concentration the trimethylsilyl-phosphaalkine could be reused for the next synthesis). The crude product was recrystallized from a *n*-pentane solution yielding the 3-benzyl-5-(trimethylsilyl)-3*H*-1,2,3,4-triazaphosphole (**1a**) as colorless solid (325 mg, 87%).

**$^{1}$H NMR (401 MHz, chloroform-*d*):** $\delta$ = 7.36 (s, 5H), 5.79 (d, $^{3}J_{P\text{-}H}$ = 6.1 Hz, 2H), 0.38 (s, 9H, $Si(CH_3)_3$) ppm.

**$^{31}$P{$^{1}$H} NMR (162 MHz, chloroform-*d*):** $\delta$ = 214.0 ppm.

**$^{13}$C NMR (101 MHz, chloroform-*d*):** $\delta$ = 185.27 (d, *J* = 75.0 Hz), 137.11, 129.08, 128.64, 128.59, 55.84 (d, *J* = 12.0 Hz), -0.26 (d, *J* = 3.5 Hz) ppm.

**ESI-TOF** (m/z): 250.0930 g/mol (calc.: 250,0923 g/mol) $[M+H]^+$.

The spectroscopic data obtained is in agreement with the literature.[4]

### 3-(2,6-diisopropylphenyl)-5-(trimethylsilyl)-3*H*-1,2,3,4-triazaphosphole (1b)

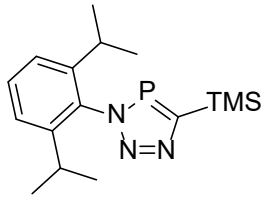


2-Azido-1,3-diisopropylbenzene (1.07 g, 5.26 mmol, 1.00 eq.) was added to an excess of trimethylsilyl-phosphaalkine in toluene. After stirring the reaction mixture overnight at room temperature, the excess of trimethylsilyl-phosphaalkine in toluene was condensed out of the reaction mixture in a separate Schlenk flask. The crude product was washed with *n*-pentane (3 x 2

mL) and the 5-rimethylsilyl-3*H*-1,2,3,4-triazaphosphole was isolated as a yellowish solid (1.39 g, 83%)

**$^{1}$H NMR (401 MHz, chloroform-*d*):** $\delta$ = 7.50 (t, *J* = 7.8 Hz, 1H, Dipp-*para*-HAr), 7.33 (d, *J* = 7.8 Hz, 2H, Dipp-*meta*-HAr), 2.10 (hept, *J* = 7.1 Hz, 2H, Dipp-*ortho*- *ipr*-CH), 1.12 (d, *J* = 6.7 Hz, 12H, Dipp-*ortho*- *ipr*-$CH_3$), 0.49 (s, 9H, C-TMS) ppm.

**$^{31}$P{$^{1}$H} NMR (162 MHz, chloroform-*d*):** $\delta$ = 223.0 ppm.

**$^{13}$C NMR (101 MHz, chloroform-*d*):** $\delta$ = 185.86 (d, *J* = 75.0 Hz), 145.96, 130.11, 123.82, 28.40, 24.41 (d, *J* = 22.8 Hz), -0.02 (d, *J* = 3.2 Hz) ppm.

**C-H-N-Analysis**: Found: C, 58.6; H, 8.8; N, 12.0. Calc. for $C_{16}H_{26}N_3PSi$: C, 60.2; H, 8.2; N, 13.1%.

**3-benzyl-1-methyl-5-(trimethylsilyl)-3*H*-1,2,3,4-triazaphosphol-1-ium tetrafluoroborate (2a)**

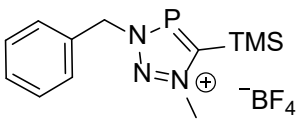


**2a** was prepared starting from **1a** (200 mg, 0.80 mmol) and trimethyloxonium tetrafluoroborate (143 mg, 0.96 mmol) in DCM (10 mL). The reaction mixture was stirred at room temperature for 2 hours, after which the solvent was removed in vacuo and the remaining solid was washed with dry diethyl ether (3 x 5 mL). **2a** was obtained as a colorless solid (222 mg, 79%).

**$^{1}$H-NMR (400 MHz, DCM-$d_2$):** $\delta$ = 7.54 – 7.50 (m, 5H), 5.82 (d, *J* = 5.6 Hz, 2H), 4.52 (s, 3H, $CH_3$), 0.53 (s, 9H, $Si(CH_3)_3$) ppm.

**$^{13}$C{$^{1}$H}-NMR (101 MHz, DCM-$d_2$):** $\delta$ = 130.9, 130.7, 130.3, 60.3, 44.7, -0.9 ppm

**$^{31}$P{$^{1}$H}-NMR (162 MHz, DCM-$d_2$):** $\delta$ = 239.3 ppm.

**$^{19}$F-NMR (377 MHz, DCM-$d_2$):** $\delta$ = − 153.2 ppm.

**$^{11}$B-NMR (129 MHz, DCM-$d_2$):** $\delta$ = − 1.5 ppm.

**ESI-TOF** (m/z): 264.1159 g/mol (calc.: 264.1086 g/mol) $[M\text{-}BF_4]^+$.

**C-H-N-Analysis**: Found: C, 40.1; H, 6.0; N, 11.2. Calc. for $C_{12}H_{19}N_3PSiBF_4$: C, 41.0; H, 5.5; N, 12.0%.

**3-(2,6-diisopropylphenyl)-1-methyl-5-(trimethylsilyl)-3H-1,2,3,4-triazaphosphol-1-ium tetrafluoroborate (2b)**

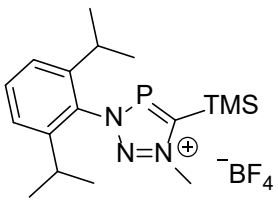


3-(2,6-diisopropylphenyl)-5-(trimethylsilyl)-3*H*-1,2,3,4-triazaphosphole (**1b**) (500 mg, 1.57 mmol) was dissolved in 10 ml DCM and trimethyloxonium tetrafluoroborate (255 mg, 1.72 mmol,) was added. The reaction mixture was stirred at room temperature overnight. Subsequently, the solvent was removed in vacuo and redissolved in acetonitrile. The solution was washed three times with 5 ml of dry diethyl ether. The solid was dried in vacuo to give product **2b** as an off white solid (636 mg, 97%).

**$^{1}$H-NMR (401 MHz DCM-$d_2$)**: $\delta$ = 7.63 (t, *J* = 7.8 Hz, 1H, Dipp-*para*-$H_{Ar}$), 7.41 (d, *J* = 7.9 Hz, 2H, Dipp-*meta*-$H_{Ar}$), 4.70 (s, 3H, N-$CH_3$), 2.21 (hept, *J* = 6.6 Hz, 2H, Dipp-*orthoipr*-CH), 1.22 (d, *J* = 6.8 Hz, 6H, Dipp-*ortho*- *ipr*-$CH_3$), 1.18 (d, *J* = 6.8 Hz, 6H, Dipp-*ortho*- *ipr*-$CH_3$), 0.71 (s, 9H, C-TMS) ppm.

**$^{13}C\{^1H\}$-NMR (101 MHz, DCM-$d_2$):** $\delta$ = 133.04, 125.34, 45.39, 29.21, 24.59, -0.63 ppm.

**$^{31}P\{^1H\}$-NMR (162 MHz, DCM-$d_2$):** $\delta$ = 249.1 ppm.

**$^{11}B$-NMR (129 MHz, DCM-$d_2$):** $\delta$ = − 1.3 ppm.

**$^{19}F$-NMR (377 MHz, DCM-$d_2$)**: $\delta$ = − 152.3 ppm.

**ESI-TOF** (m/z): 262.1476 g/mol (calc.: 262.1468 g/mol) $[M\text{-}SiMe_3BF_4]^+$, 334.1871 g/mol (calc.: 334.1868 g/mol) $[M\text{-}BF_4]^+$.

**C-H-N-Analysis**: Found: C, 48.3; H, 7.3; N, 10.0. Calc. for $C_{17}H_{29}N_3PSiBF_4$: C, 49.7; H, 7.2; N, 9.7%.

**3-benzyl-1-methyl-3H-1,2,3,4-triazaphosphol-1-ium tetrafluoroborate (3a)**

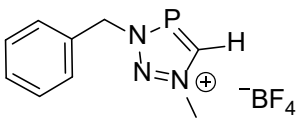

The corresponding triazaphospholenium salt **2a** (200 mg, 0.57 mmol) was dissolved in DME (10 mL) and stirred at *T* = 60°C for 4 days. Subsequently, the solvent was removed in vacuo. After washing with *n*-pentane (3 x 5 mL)**3a** was obtained as a colorless oil (84 mg, 53%).

**$^1H$-NMR (401 MHz, acetonitrile-$d_3$):** $\delta$ = 9.33 (d, *J* = 37.5 Hz, 1H), 7.56 – 7.41 (m, 5H), 5.81 (d, $^3J_{P\text{-}H}$ = 6.0 Hz, 2H), 4.42 (s, 3H) ppm.

**$^{13}C\{^1H\}$-NMR (101 MHz, acetonitrile-$d_3$):** $\delta$ = 165.0 (d, *J* = 62.3 Hz, C=P), 131.0 ($C_{Ar}$), 130.8 ($C_{Ar}$), 130.5 ($C_{Ar}$), 72.66 ($CH_2$), 44.5 ($CH_3$) ppm.

**$^{31}P\{^1H\}$-NMR (162 MHz, acetonitrile-$d_3$):** $\delta$ = 206.7 ppm.

**$^{11}B$-NMR (129 MHz, acetonitrile-$d_3$):** $\delta$ = − 0.3 ppm.

**$^{19}F$-NMR (377 MHz, acetonitrile-$d_3$):** $\delta$ = − 150.7 ppm.

**(3-benzyl-1-methyl-3H-1,2,3,4-triazaphosphol-1-ium-5-yl)trifluoroborate (4a)**

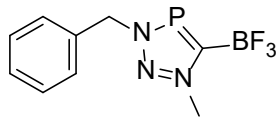

The corresponding triazaphospholenium salt **2a** (134.0 mg, 0.38 mmol) was dissolved in DME (5 mL) and stirred at *T* = 60 °C for 6 hours. Subsequently, the solvent was removed under high vacuum, and the crude product was purified by column chromatography in hexane : ethyl acetate (1 : 9). **4a** was obtained as a colorless oil (45 mg, 42%).

**$^1H$-NMR (401 MHz, DCM-$d_2$):** $\delta$ = 7.69 – 7.31 (m, 5H), 5.68 (d, *J* = 5.6 Hz, 2H), 4.47 (d, *J* = 0.9 Hz, 3H) ppm.

**$^{13}C\{^1H\}$-NMR (101 MHz, DCM-$d_2$):** $\delta$ = 133.9 (d, *J* =49.7 Hz), 130.5 ($C_{Ar}$), 130.1 ($C_{Ar}$), 129.7 ($C_{Ar}$), 59.8 (d, *J* = 10.0 Hz, $CH_2$), 42.8 ($CH_3$) ppm.

**$^{31}P\{^1H\}$-NMR (162 MHz, DCM-$d_2$):** $\delta$ = 229.3 ppm.

**$^{11}B$-NMR (129 MHz, DCM-$d_2$):** $\delta$ = 0.65 (qd, *J* = 37.9, 15.9 Hz) ppm.

**$^{19}F$-NMR (377 MHz, DCM-$d_2$):** $\delta$ = − 140.5 (qd, *J* = 37.7, 14.6 Hz) ppm.

**(3-(2,6-diisopropylphenyl)-1-methyl-3*H*-1,2,3,4-triazaphosphol-1-ium-5-yl)trifluoroborate (4b)**

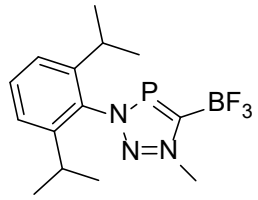

The corresponding triazaphospholenium salt **2b** (136 mg, 0.31 mmol) was dissolved in DME (2 mL), and stirred at *T* = 60 °C for 2 hours. Subsequently, the solvent was removed under high vacuum, and the crude product was purified by column chromatography in hexane : ethyl acetate (1 : 9). **4b** was obtained as a yellowish oil.

**$^{1}$H-NMR (401 MHz, THF-*d*$_8$):** $\delta$ = 7.66 (t, *J* = 3.0 Hz, 1H),7.49 (d, *J* = 7.8 Hz, 2H), 3.32 (s, 3H, N-$CH_3$), 2.46 (hept, *J* = 6.8 Hz, 2H), 1.25 (d, *J* = 6.8 Hz, 12H) ppm.

**$^{13}$C-NMR (101 MHz, THF-*d*$_8$):** $\delta$ = 146.2 ($C_{Ar}$), 145.7 ($C_{Ar}$), 132.4 ($C_{Ar}$), 124.9 ($C_{Ar}$), 72.5 (C=P), 44.1 (N-CH3), 28.9 (isopropyl), 24.1 (isopropyl) ppm.

**$^{31}$P{$^{1}$H}-NMR (162 MHz, THF-*d*$_8$):** $\delta$ = 240.1 ppm.

**$^{11}$B-NMR (129 MHz, THF-*d*$_8$):** $\delta$ = 0.6 (qd, *J* = 37.8, 15.3 Hz) ppm.

**$^{19}$F-NMR-Spektrum (377 MHz, DCM-*d*$_2$)**: $\delta$ = − 140.4 (qd, *J* = 72.0, 14.3 Hz) ppm.

**C-H-N-Analysis**: Found: C, 49.4; H, 6.4; N, 10.2. Calc. for $C_{14}H_{20}N_3PBF_3$: C, 51.1; H, 6.1; N, 12.8%.

**3-benzyl-1-ethyl-5-(trimethylsilyl)-3*H*-1,2,3,4-triazaphosphol-1-ium hexafluorophosphate (5a)**

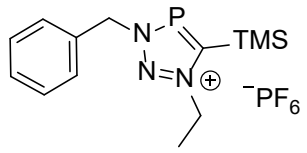

Triazaphosphol **1a** (300 mg, 1.20 mmol) and triethyloxonium hexafluorophosphate (298 mg, 1.20 mmol) were dissolved in DCM (10 mL) and stirred for two hours at room temperature. Removal of the solvent in vacuum gave the crude product which was purified by washing with *n*-pentane (3 x 3 mL) followed by drying the solid in vacuo. **5a** was obtained as a yellowish solid (407 mg, 80%).

**$^{1}$H-NMR (401 MHz, chloroform-*d*):** $\delta$ = 7.71 – 7.37 (m, 5H, $H_{Ar}$), 5.83 (d, *J* = 5.5 Hz,2H), 4.80 (q, *J* = 7.3 Hz, 2H, N-$CH_2$), 1.83 (t, *J* = 7.3 Hz, 3H, N-$CH_2$-$CH_3$), 0.57 (s, 9H, C-TMS) ppm.

**$^{31}$P{$^{1}$H}-NMR (162 MHz, chloroform-*d*):** $\delta$ = 238.3 (s, P=C), − 144.9 (hept, *J* = 712.9 Hz, $PF_6$) ppm.

**$^{19}$F-NMR (377 MHz, chloroform-*d*):** = -73.3 (d, *J* = 713.0 Hz) ppm.

**$^{13}$C NMR (101 MHz, chloroform-*d*):** δ = 181.3 (d, *J* = 61.6 Hz), 132.6, 130.9, 130.4, 60.4, 54.2, -0.4 (d, *J* = 6.4 Hz) ppm.

**ESI-TOF** (m/z): 278.1285 g/mol (calc.: 278.1242 g/mol) $[M\text{-}PF_6]^+$.

**3-(2,6-diisopropylphenyl)-1-ethyl-5-(trimethylsilyl)-3*H*-1,2,3,4-triazaphosphol-1-ium hexafluorophosphate (5b)**

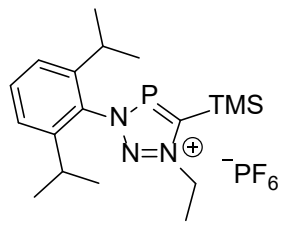

Triazaphosphol **1b** (1.73 g, 5.42 mmol) was dissolved in 10 ml DCM and triethyloxonium hexafluorophosphate (1.23 g, 4.92 mmol) was added. The reaction mixture was stirred overnight. Subsequently, the solvent was removed in vacuo and dissolved in acetonitrile. The solution was washed three times with 5 ml of *n*-pentane. The solvent of the acetonitrile fraction

was removed in vacuo and product **5b** was obtained as a colorless solid (2.26 g, 93%).

**$^{1}$H-NMR (400 MHz, DCM-*d*$_2$):** $\delta$ = 7.66 (t, *J* = 7.8 Hz, 1H), 7.43 (d, *J* = 7.9 Hz, 2H), 4.95 (q, *J* = 7.3 Hz, 2H), 2.19 (p, *J* = 6.9 Hz, 2H), 1.78 (t, *J* = 7.2 Hz, 3H), 1.24 (d, *J* = 6.8 Hz, 6H), 1.17 (d, *J* = 6.7 Hz, 6H), 0.70 (s, 9H)ppm.

**$^{31}$P{$^{1}$H}-NMR (162 MHz, DCM-*d*$_2$):** $\delta$ = 248.7 (s, P=C), 144.0 (hept, *J* = 711.6 Hz, $PF_6$) ppm.

**$^{19}$F-NMR (377 MHz, DCM-*d*$_2$):** = -72.8 (d, *J* = 719.1 Hz) ppm.

**$^{13}$C NMR (101 MHz, DCM-*d*$_2$):** δ = 145.7, 133.1, 125.4, 55.2, 29.4, 24.8, 24.3, 15.9, -0.4 ppm.

**C-H-N-Analysis**: Found: C, 44.5; H, 6.8; N, 8.9. Calc. for $C_{18}H_{31}N_3P_2SiF_6$: C, 43.8; H, 6.3; N, 8.5%.

**3-(2,6-diisopropylphenyl)-1-ethyl-3*H*-1,2,3,4-triazaphosphol-1-ium hexafluorophosphate (6b)**

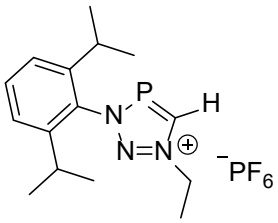


The triazaphospholenium Salt **5b** (200 mg, 0.41 mmol) and potassium fluoride (118 mg, 2.03 mmol) were dissolved in DCM (5 mL) and stirred at *T* = -78°C for overnight. After adding *n*-pentane (3 mL) the precipitate was filtered of and the remaining solution dried in vacuo. The product **6b** was obtained as yellow solid (75 mg, 44%).

**$^{1}$H-NMR (401 MHz, DCM-*d*$_2$):** $\delta$ = 9.91 (d, *J* = 35.9 Hz, 1H), 7.65 (t, *J* = 7.9 Hz, 1H), 7.42 (d, *J* = 7.9 Hz, 2H), 5.00 (q, *J* = 7.5 Hz, 2H), 2.17 (hept, *J* = 6.8 Hz, 2H), 1.78 (t, *J* = 7.3 Hz, 3H), 1.23 (dd, *J* = 29.6, 6.8 Hz, 12H) ppm.

**$^{31}$P{$^{1}$H}-NMR (162 MHz, DCM-*d*$_2$):** $\delta$ = 214.4 (s, P=C), − 144.4 (hept, *J* =711.6 Hz, $PF_6$) ppm.

**$^{19}$F-NMR (377 MHz, DCM-*d*$_2$):** $\delta$ = − 72.1 (d, *J* = 711.6 Hz) ppm.

**$^{13}$C{$^{1}$H}-NMR (101 MHz, DCM-*d*$_2$):** $\delta$ = 165.3 (C=P), 145.7 ($C_{Ar}$), 145.7 ($C_{Ar}$), 133.2 ($C_{Ar}$), 125.3($C_{Ar}$), 54.8 (N-$CH_2$), 29.4 (N-$CH_2$-$CH_3$), 24.7 (isopropyl), 24.2 (isopropyl), 15.3 (isopropyl) ppm.

**(3-(2,6-diisopropylphenyl)-1-ethyl-3*H*-1,2,3,4-triazaphosphol-1-ium-5-yl)triethylborate (7b)**

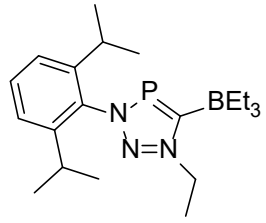


The triazaphospholenium salt **5b** (300 mg, 0.61 mmol) was added together with the potassium fluoride (70.6 mg, 1,22 mmol) and then dissolved in dry THF (5 mL). The reaction mixture was cooled to *T* = − 78°C and carefully 0.9 mL of a 1 M solution of $BEt_3$ in THF (71.5 mg, 0.73 mmol) was added. The reaction mixture was allowed to warm to room temperature overnight. The solvent was removed in vacuo, dry DCM (3 mL) was added, and the solution was filtered. The product **7b** was obtained from the solution after removal of the solvent in vacuum as pale yellow oil (111 mg, 49%).

**$^{1}$H-NMR (401 MHz, DCM-*d*$_2$):** $\delta$ = 7.54 (t, *J* = 7.9 Hz, 1H), 7.34 (d, *J* = 7.9 Hz, 2H), 4.89 (q, *J* = 7.3 Hz, 2H, N-$CH_2$), 2.20 (hept, *J* = 6.8 Hz, 2H), 1.59 – 1.57 (m, 3H, N-$CH_2$-$CH_3$), 1.20 (d, *J* = 6.8 Hz, 6H), 1.12 (d, *J* = 6.9 Hz, 6H), 0.69 (t, J = 7.5 Hz, 9H, B-$CH_2$-$CH_3$), 0.44 (q, *J* = 7.6 Hz, 6H, B-$CH_2$) ppm.

**$^{31}$P{$^{1}$H}-NMR (162 MHz, DCM-*d*$_2$):** $\delta$ = 242.9 (s) ppm.

**$^{11}$B-NMR (129 MHz, DCM-*d*$_2$):** $\delta$ = − 13.5 (s) ppm.

**$^{13}C\{^1H\}$-NMR (101 MHz, DCM-$d_2$):** $\delta$ = 177.7, 145.6, 131.6, 124.7, 71.1, 50.9, 27.2, 24.7, 24.3 (d, $J$ = 39.8 Hz), 16.3, 11.0 ppm.

## 2. Additional Figures

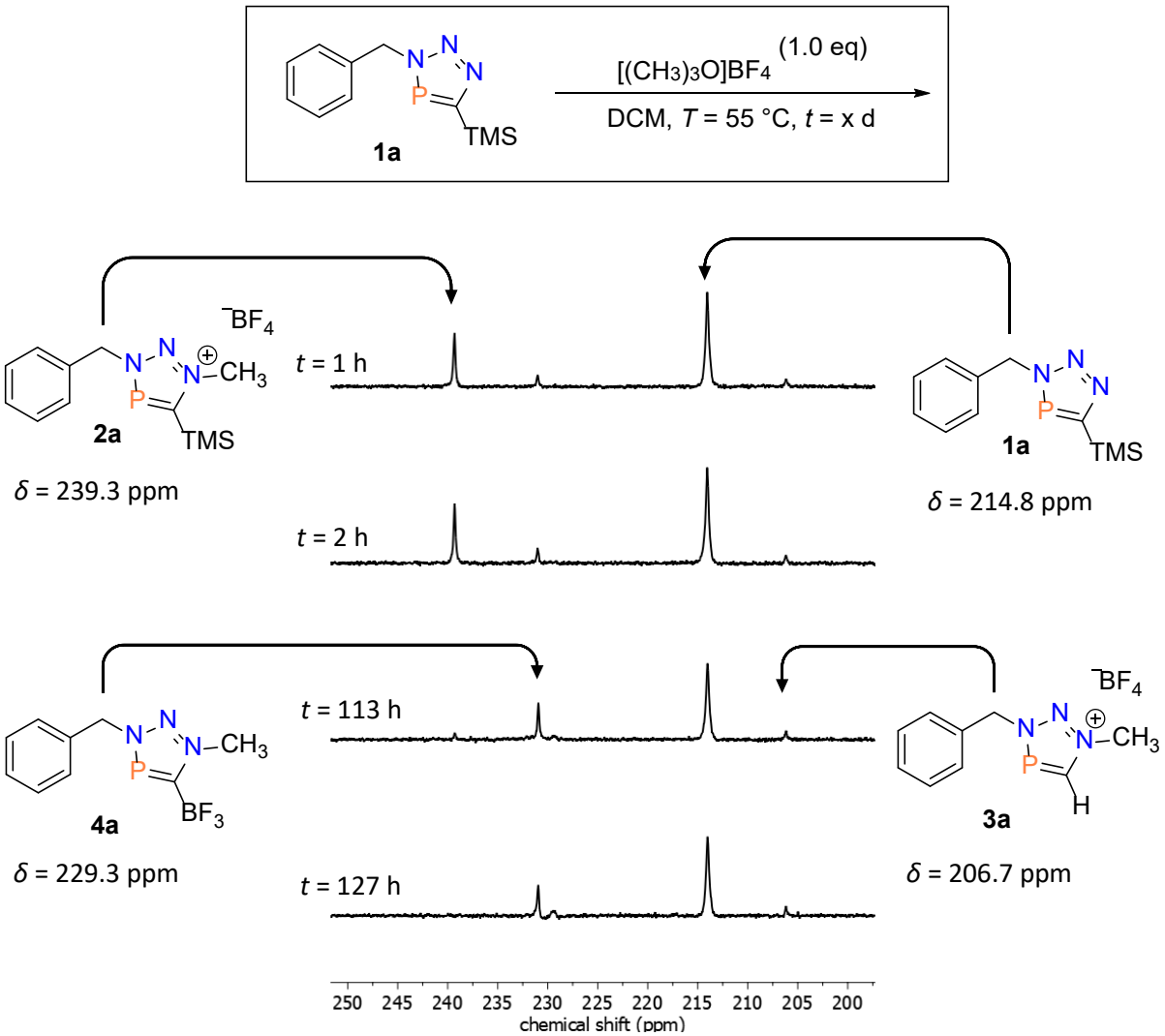


**Figure S1**: Monitoring the reaction progress by $^{31}P\{^{1}H\}$-NMR spectroscopy (without solvent) of the attempted preparation of quaternized 3*H*-1,2,3,4-triazaphosphole **1a**.

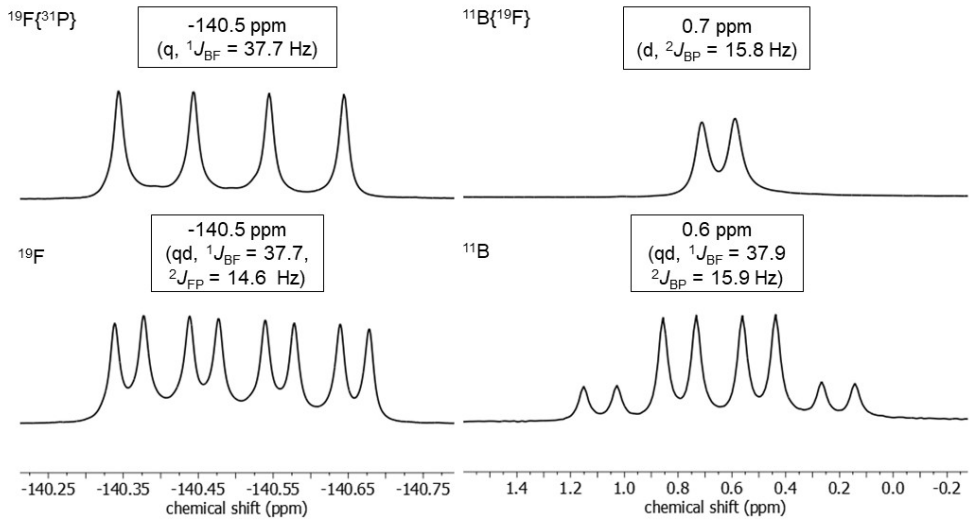


**Figure S2**: $^{11}B$ and $^{19}F$ NMR spectra of $BF_3$-3*H* 1,2,3,4 triazaphospholenium salt adduct **4a** in MeCN-$d_3$.

## 3. Crystallographic Details

X-ray studies were carried out on a D8 Venture, Bruker Photon CMOS diffractometer[5] (MoKα radiation; λ = 0.71073 Å and CuKα radiation; λ = 1.54178 Å) up to a resolution of (sinΘ/λ) max = 0.58 Å (6) 0.60 Å (3, 9) at 100(2) K. The structures of were solved with SHELXT-2018[6] by using direct methods and refined with SHELXL-2018/3 [7] on F2 for all reflections. Non-hydrogen atoms were refined by using anisotropic displacement parameters. The positions of the hydrogen atoms were calculated for idealized positions. Geometry calculations and checks for higher symmetry were performed with the PLATON program.[8] The program Olex2 [9] was also used to aid in the refinement of the structures of compounds. All non-hydrogen atoms were refined anisotropically. All hydrogen atoms were included into the model at geometrically calculated positions and refined using a riding model. The isotropic displacement parameter of all hydrogen atoms were fixed to 1.2 times the U-value of the atoms they are linked to (1.5 times for methyl groups). Crystallographic data for the structures reported in this paper have been deposited in the Cambridge Crystallographic Database Center: CCDC number: 2279457(**3a**) 2279453(**4a**), 2279454(**4b**), 2279455 (**6b**) 2279456 (**7b**). Details of the X-ray structure determinations and refinements are provided in Table S1-S5.

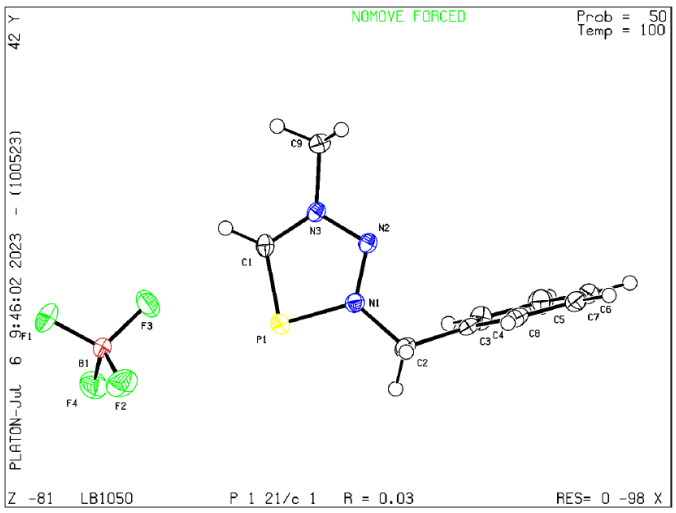


Table S1 Crystal data and structure refinement for **3a**.

| | |
|---|---|
| Identification code | LB1050 |
| Empirical formula | $C_9H_{11}BF_4N_3P$ |
| Formula weight | 278.999 |
| Temperature/K | 100.00 |
| Crystal system | monoclinic |
| Space group | $P2_1/c$ |
| a/Å | 10.71411(7) |
| b/Å | 8.96879(6) |
| c/Å | 13.55016(9) |
| α/° | 90 |
| β/° | 111.9100(2) |
| γ/° | 90 |
| Volume/Å$^3$ | 1208.023(14) |
| Z | 4 |
| $\rho_{calc}$g/cm$^3$ | 1.534 |
| μ/mm$^{-1}$ | 2.400 |
| F(000) | 571.6 |
| Crystal size/mm$^3$ | 0.7 × 0.16 × 0.05 |
| Radiation | Cu Kα (λ = 1.54178) |
| 2Θ range for data collection/° | 8.9 to 136.56 |
| Index ranges | $-12 \le h \le 12$, $-10 \le k \le 10$, $-16 \le l \le 16$ |
| Reflections collected | 18430 |
| Independent reflections | 2174 [$R_{int}$ = 0.0343, $R_{sigma}$ = 0.0205] |
| Data/restraints/parameters | 2174/0/164 |
| Goodness-of-fit on $F^2$ | 1.062 |
| Final R indexes [I>=2σ (I)] | $R_1$ = 0.0301, $wR_2$ = 0.0771 |
| Final R indexes [all data] | $R_1$ = 0.0311, $wR_2$ = 0.0779 |
| Largest diff. peak/hole / e Å$^{-3}$ | 0.29/-0.31 |

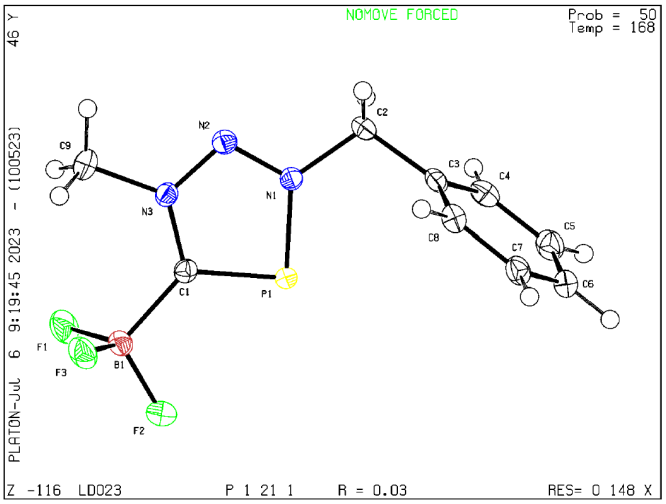


Table S2 Crystal data and structure refinement for **4a**

| | |
|---|---|
| Identification code | LD023 |
| Empirical formula | $C_9H_{10}BF_3N_3P$ |
| Formula weight | 258.993 |
| Temperature/K | 168.00 |
| Crystal system | monoclinic |
| Space group | $P2_1$ |
| a/Å | 5.80174(8) |
| b/Å | 8.60271(12) |
| c/Å | 11.79661(16) |
| α/° | 90 |
| β/° | 99.5596(5) |
| γ/° | 90 |
| Volume/Å$^3$ | 580.601(14) |
| Z | 2 |
| $\rho_{calc}$g/cm$^3$ | 1.481 |
| μ/mm$^{-1}$ | 0.255 |
| F(000) | 264.4 |
| Crystal size/mm$^3$ | 0.49 × 0.17 × 0.15 |
| Radiation | Mo Kα (λ = 0.71073) |
| 2Θ range for data collection/° | 5.88 to 52.76 |
| Index ranges | $-7 \le h \le 7$, $-10 \le k \le 10$, $-14 \le l \le 14$ |
| Reflections collected | 14658 |
| Independent reflections | 2376 [$R_{int}$ = 0.0304, $R_{sigma}$ = 0.0253] |
| Data/restraints/parameters | 2376/1/155 |
| Goodness-of-fit on F$^2$ | 1.159 |
| Final R indexes [I>=2σ (I)] | $R_1$ = 0.0261, $wR_2$ = 0.0590 |
| Final R indexes [all data] | $R_1$ = 0.0264, $wR_2$ = 0.0594 |
| Largest diff. peak/hole / e Å$^{-3}$ | 0.51/-0.32 |
| Flack parameter | -0.00(2) |

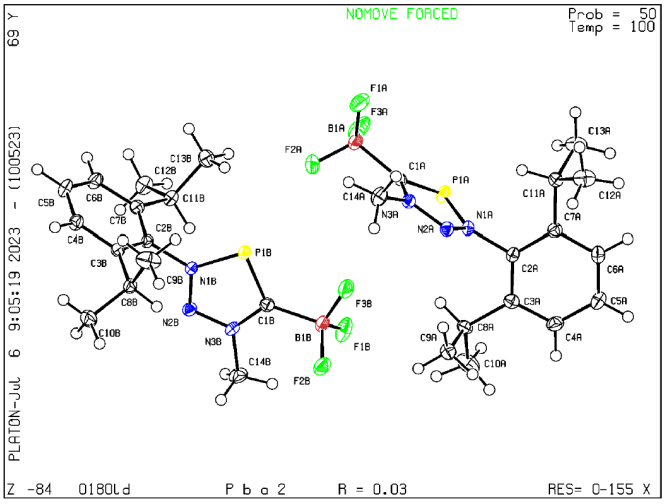


Table S3 Crystal data and structure refinement for **4b**.

| | |
|---|---|
| Identification code | 0180LD |
| Empirical formula | $C_{14}H_{20}BF_3N_3P$ |
| Formula weight | 329.11 |
| Temperature/K | 100.0 |
| Crystal system | orthorhombic |
| Space group | Pba2 |
| a/Å | 11.2355(2) |
| b/Å | 30.5407(5) |
| c/Å | 9.5592(2) |
| α/° | 90 |
| β/° | 90 |
| γ/° | 90 |
| Volume/Å$^3$ | 3280.14(10) |
| Z | 8 |
| $\rho_{calc}$g/cm$^3$ | 1.333 |
| μ/mm$^{-1}$ | 0.196 |
| F(000) | 1376.0 |
| Crystal size/mm$^3$ | 0.31 × 0.25 × 0.11 |
| Radiation | MoKα (λ = 0.71073) |
| 2Θ range for data collection/° | 3.862 to 51.426 |
| Index ranges | -13 ≤ h ≤ 13, -37 ≤ k ≤ 37, -11 ≤ l ≤ 11 |
| Reflections collected | 41596 |
| Independent reflections | 6034 [$R_{int}$ = 0.0321, $R_{sigma}$ = 0.0211] |
| Data/restraints/parameters | 6034/1/408 |
| Goodness-of-fit on F$^2$ | 1.047 |
| Final R indexes [I>=2σ (I)] | $R_1$ = 0.0270, $wR_2$ = 0.0676 |
| Final R indexes [all data] | $R_1$ = 0.0286, $wR_2$ = 0.0688 |
| Largest diff. peak/hole / e Å$^{-3}$ | 0.27/-0.18 |
| Flack parameter | 0.03(2) |

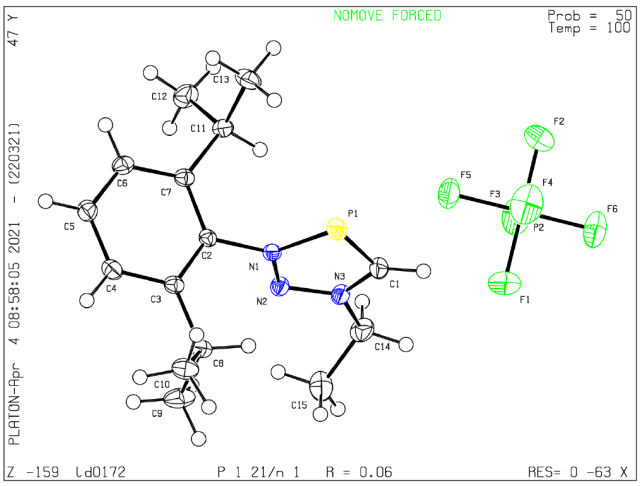


Table S4 Crystal data and structure refinement for **6b**.

| | |
|---|---|
| Identification code | LD0172 |
| Empirical formula | $C_{15}H_{23}F_6N_3P_2$ |
| Formula weight | 421.30 |
| Temperature/K | 99.95 |
| Crystal system | monoclinic |
| Space group | $P2_1/n$ |
| a/Å | 10.3822(4) |
| b/Å | 8.4426(2) |
| c/Å | 21.5901(7) |
| α/° | 90 |
| β/° | 95.4340(10) |
| γ/° | 90 |
| Volume/Å$^3$ | 1883.93(10) |
| Z | 4 |
| $\rho_{calc}$g/cm$^3$ | 1.485 |
| μ/mm$^{-1}$ | 0.292 |
| F(000) | 872.0 |
| Crystal size/mm$^3$ | 0.219 × 0.167 × 0.046 |
| Radiation | MoKα (λ = 0.71073) |
| 2Θ range for data collection/° | 4.208 to 61.054 |
| Index ranges | -14 ≤ h ≤ 14, -11 ≤ k ≤ 12, -30 ≤ l ≤ 29 |
| Reflections collected | 44368 |
| Independent reflections | 5744 [$R_{int}$ = 0.0467, $R_{sigma}$ = 0.0279] |
| Data/restraints/parameters | 5744/0/240 |
| Goodness-of-fit on F$^2$ | 1.048 |
| Final R indexes [I>=2σ (I)] | $R_1$ = 0.0597, w$R_2$ = 0.1619 |
| Final R indexes [all data] | $R_1$ = 0.0712, w$R_2$ = 0.1711 |
| Largest diff. peak/hole / e Å$^{-3}$ | 1.17/-0.67 |

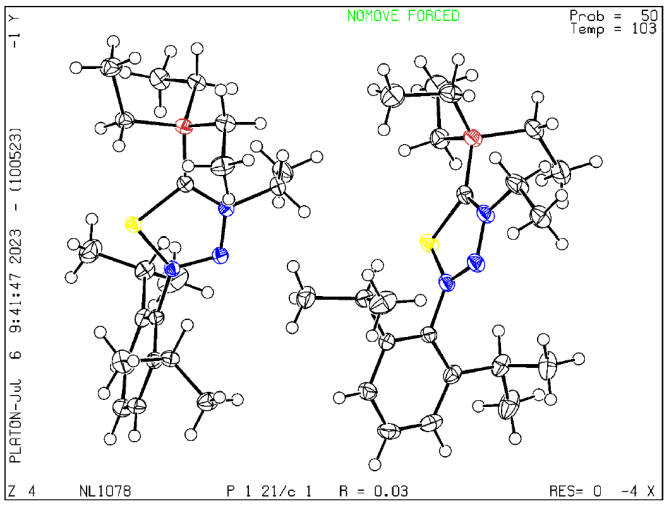


Table S5 Crystal data and structure refinement for **7b**.

| | |
|---|---|
| Identification code | NL1078 |
| Empirical formula | $C_{21}H_{37}BN_3P$ |
| Formula weight | 373.346 |
| Temperature/K | 102.60 |
| Crystal system | monoclinic |
| Space group | $P2_1/c$ |
| a/Å | 14.06027(9) |
| b/Å | 23.24206(15) |
| c/Å | 14.36186(9) |
| α/° | 90 |
| β/° | 102.7284(2) |
| γ/° | 90 |
| Volume/Å$^3$ | 4577.97(5) |
| Z | 8 |
| $\rho_{calc}$g/cm$^3$ | 1.083 |
| μ/mm$^{-1}$ | 1.110 |
| F(000) | 1638.6 |
| Crystal size/mm$^3$ | 0.3 × 0.23 × 0.12 |
| Radiation | Cu Kα (λ = 1.54178) |
| 2Θ range for data collection/° | 6.44 to 149.32 |
| Index ranges | $-17 \leq h \leq 17$, $-29 \leq k \leq 27$, $-17 \leq l \leq 17$ |
| Reflections collected | 78829 |
| Independent reflections | 9356 [$R_{int}$ = 0.0378, $R_{sigma}$ = 0.0201] |
| Data/restraints/parameters | 9356/0/485 |
| Goodness-of-fit on F$^2$ | 1.033 |
| Final R indexes [I>=2σ (I)] | $R_1$ = 0.0327, $wR_2$ = 0.0874 |
| Final R indexes [all data] | $R_1$ = 0.0348, $wR_2$ = 0.0896 |
| Largest diff. peak/hole / e Å$^{-3}$ | 0.35/-0.24 |

## 4. NMR Spectroscopic Data

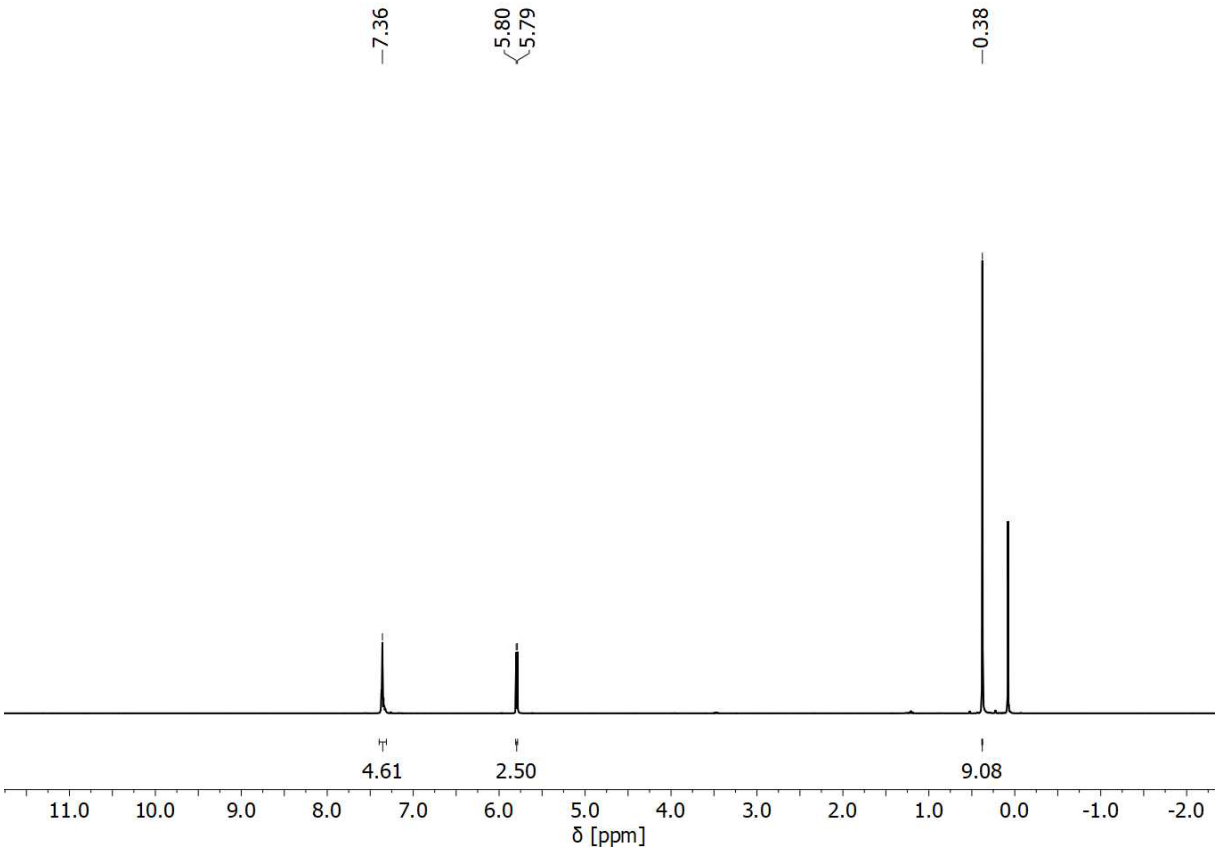


**Figure S3:** $^{1}$H NMR spectrum of **1a**.

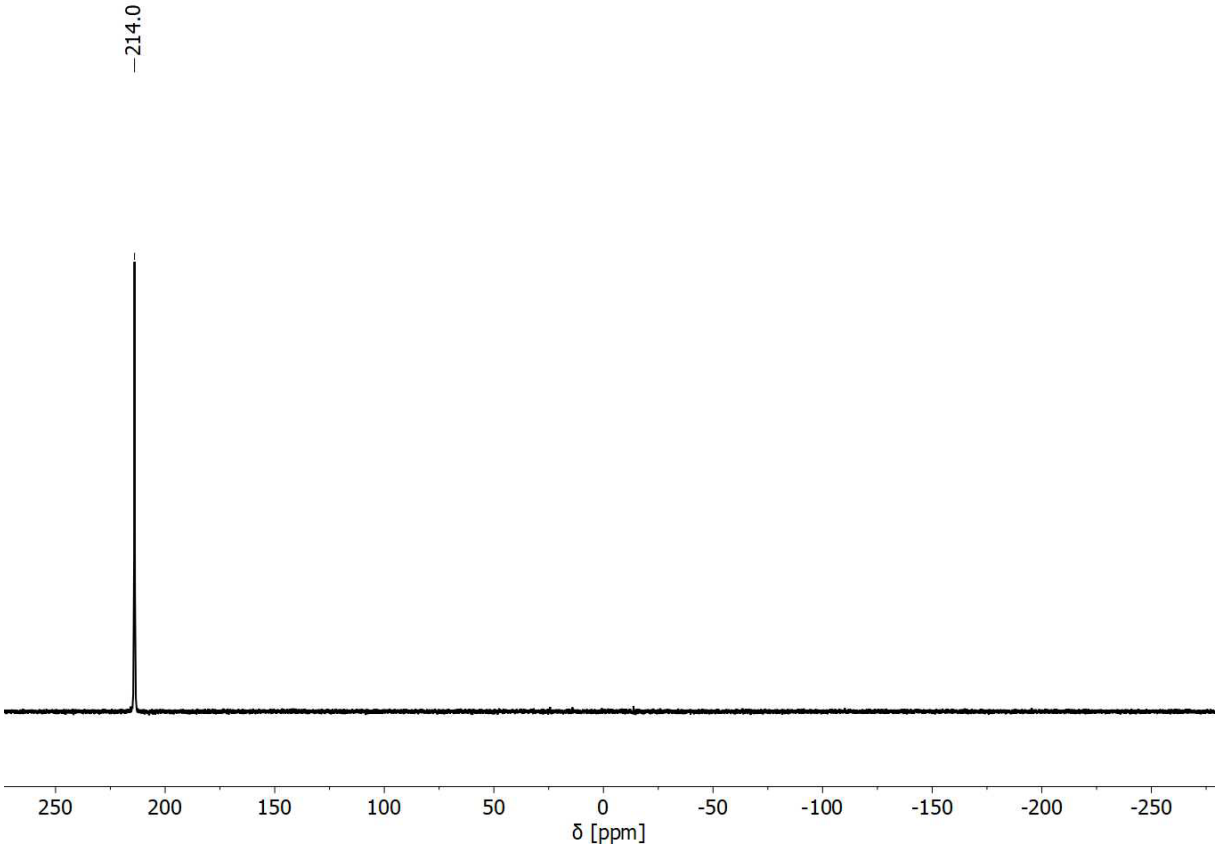


**Figure S4**: $^{31}P\{^{1}H\}$ NMR spectrum of **1a.**

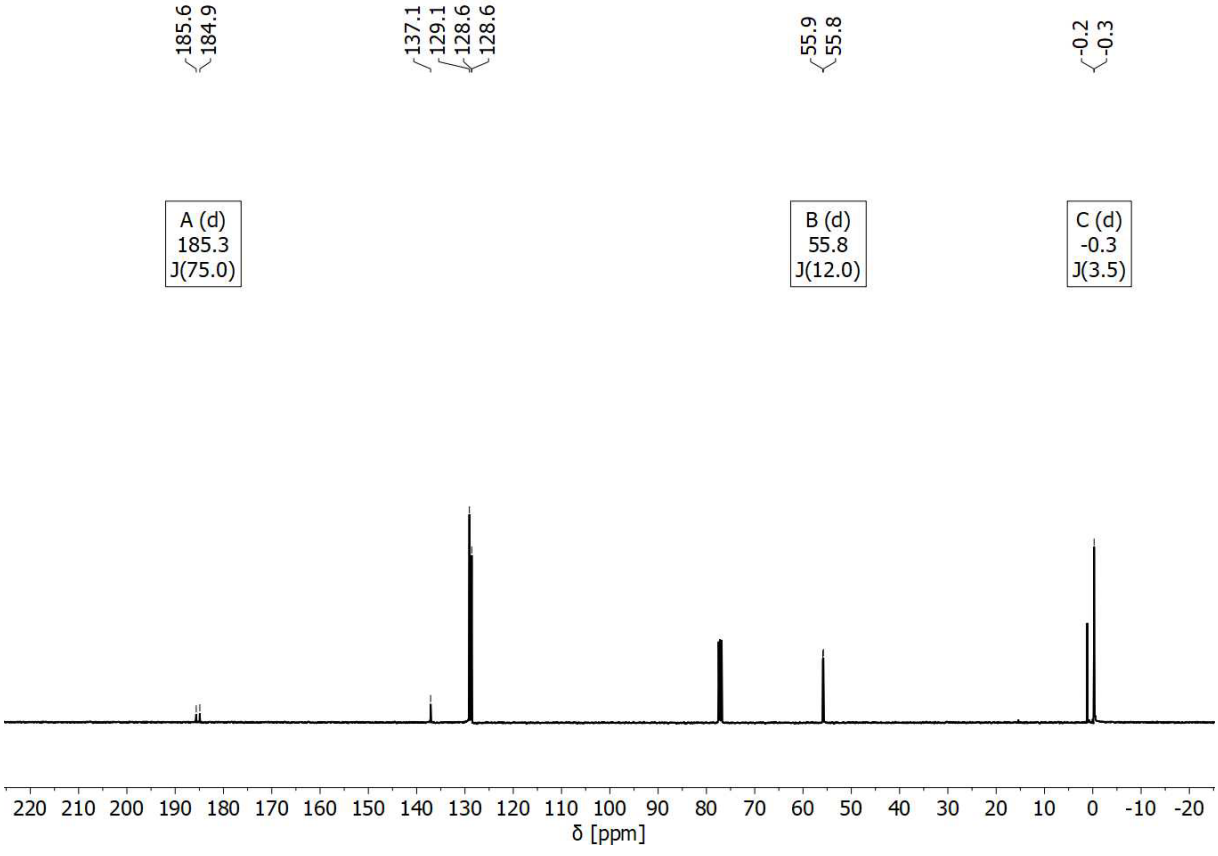


**Figure S5**: $^{13}C$ NMR spectrum of **1a.**

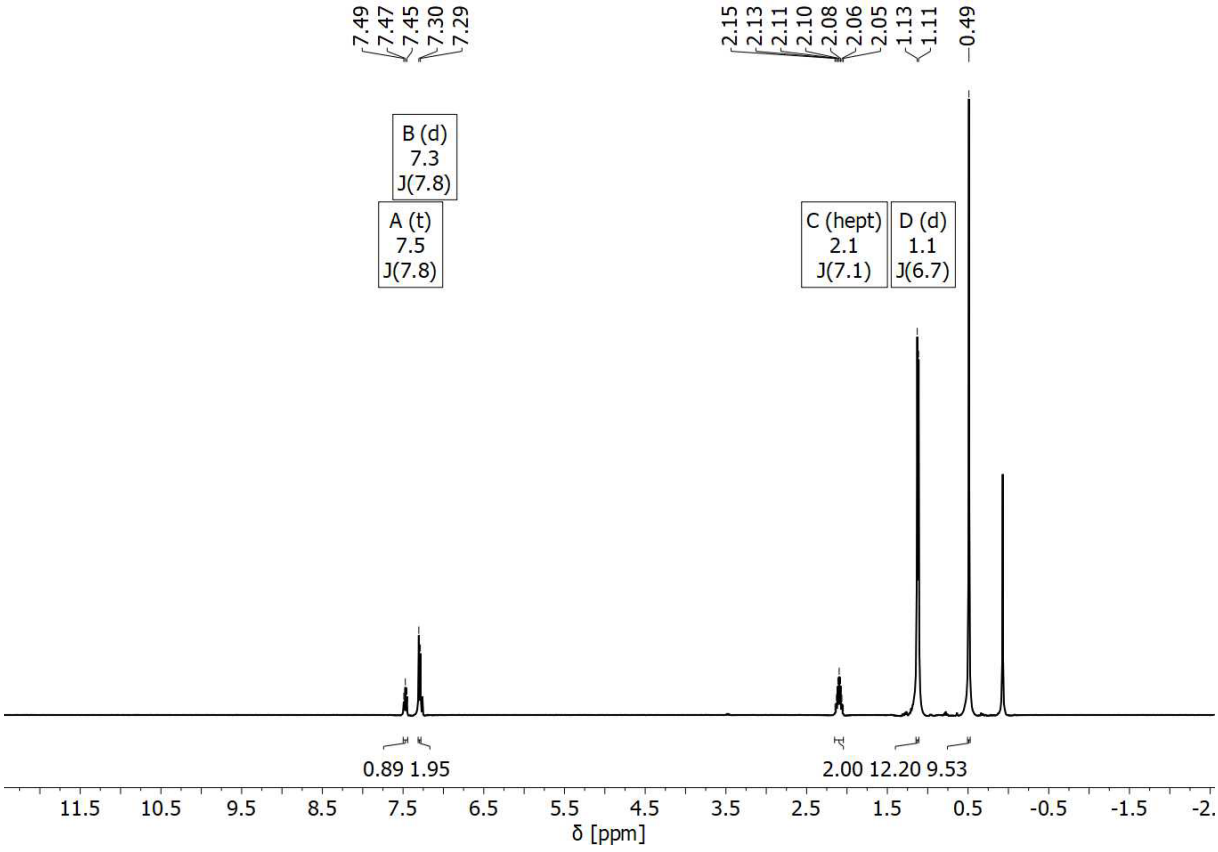


**Figure S6:** $^{1}H$ NMR spectrum of **1b**.

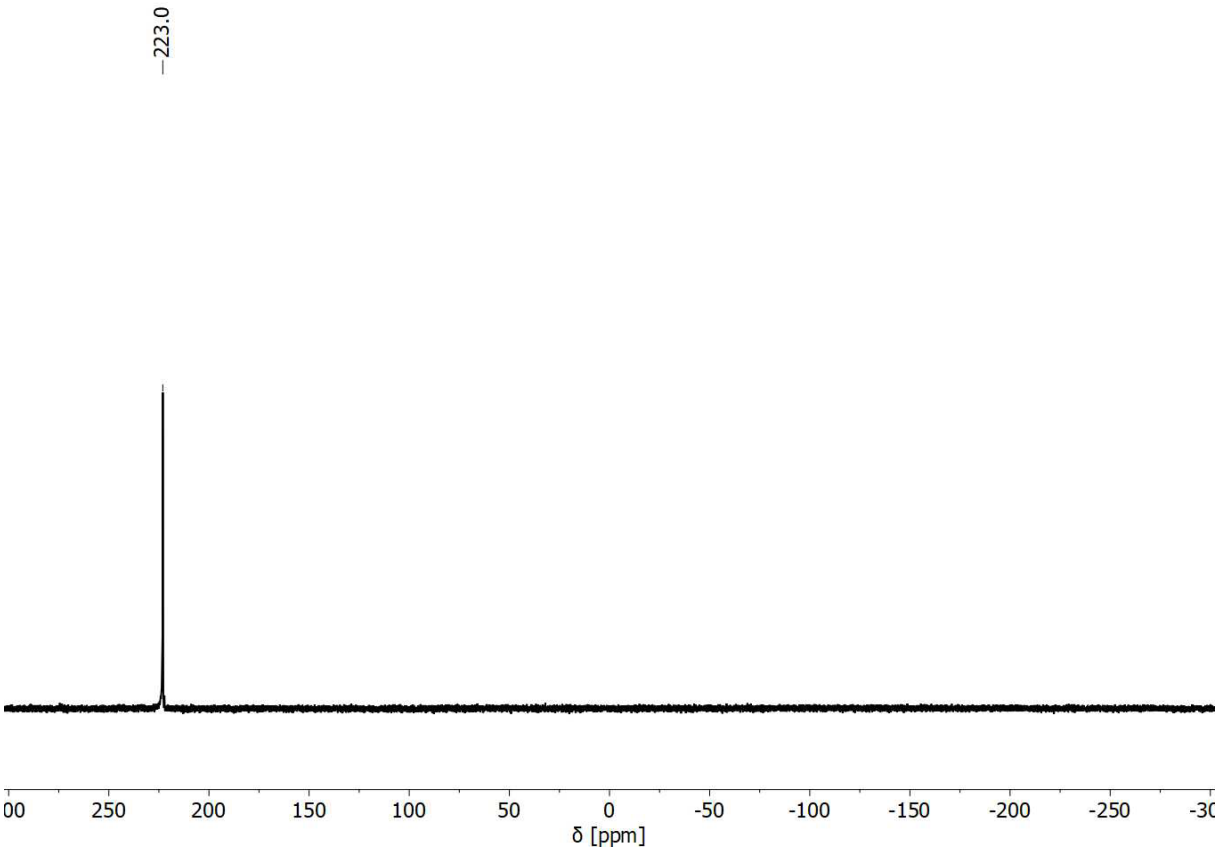


**Figure S7**: $^{31}P\{^{1}H\}$ NMR spectrum of **1b.**

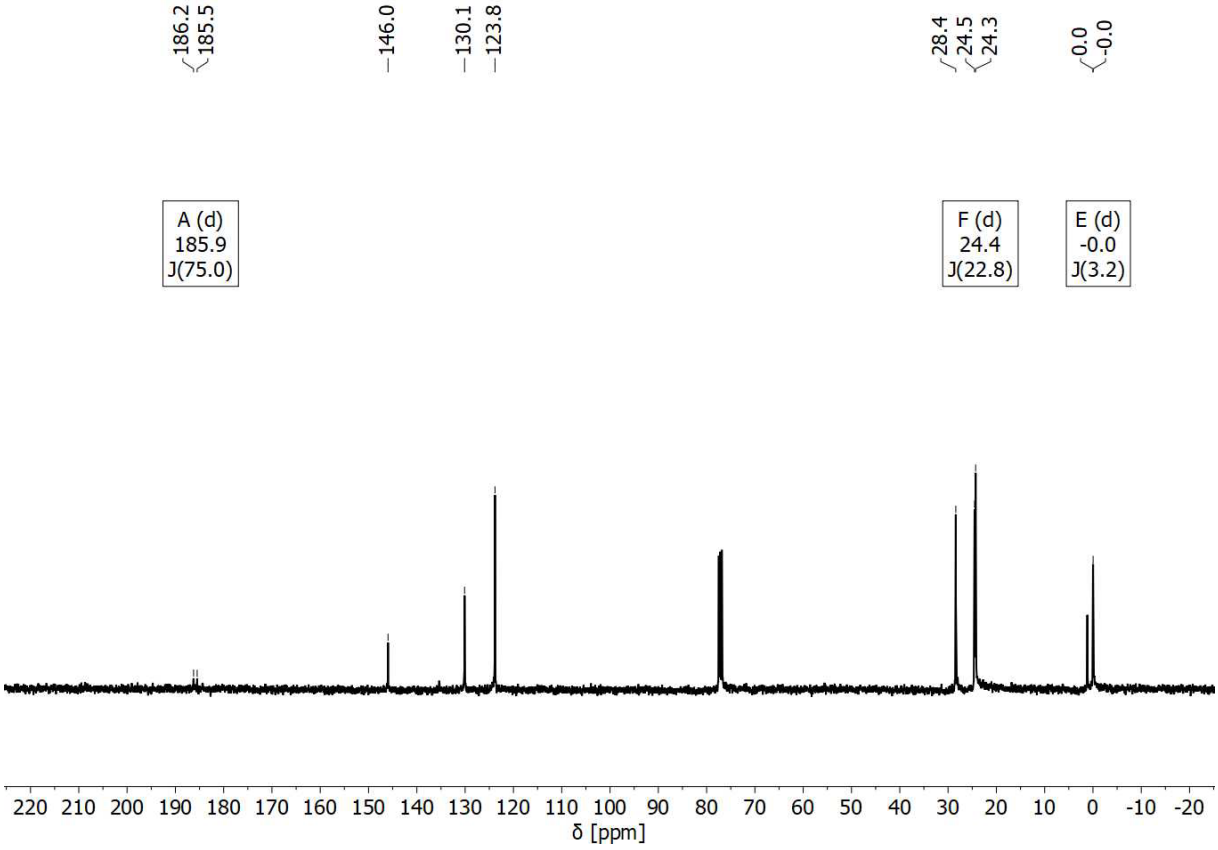


**Figure S8**: $^{13}C$ NMR spectrum of **1b.**

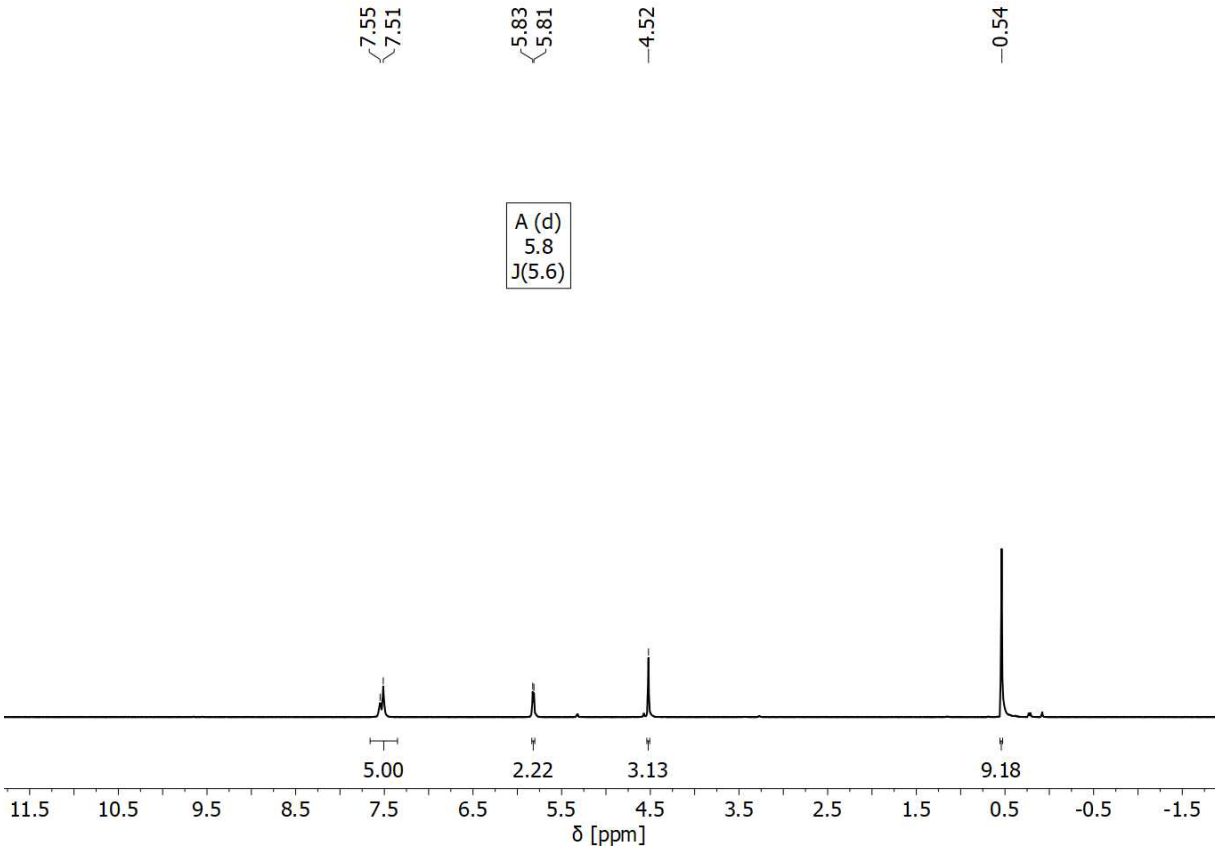


**Figure S9:** $^{1}H$ NMR spectrum of **2a**.

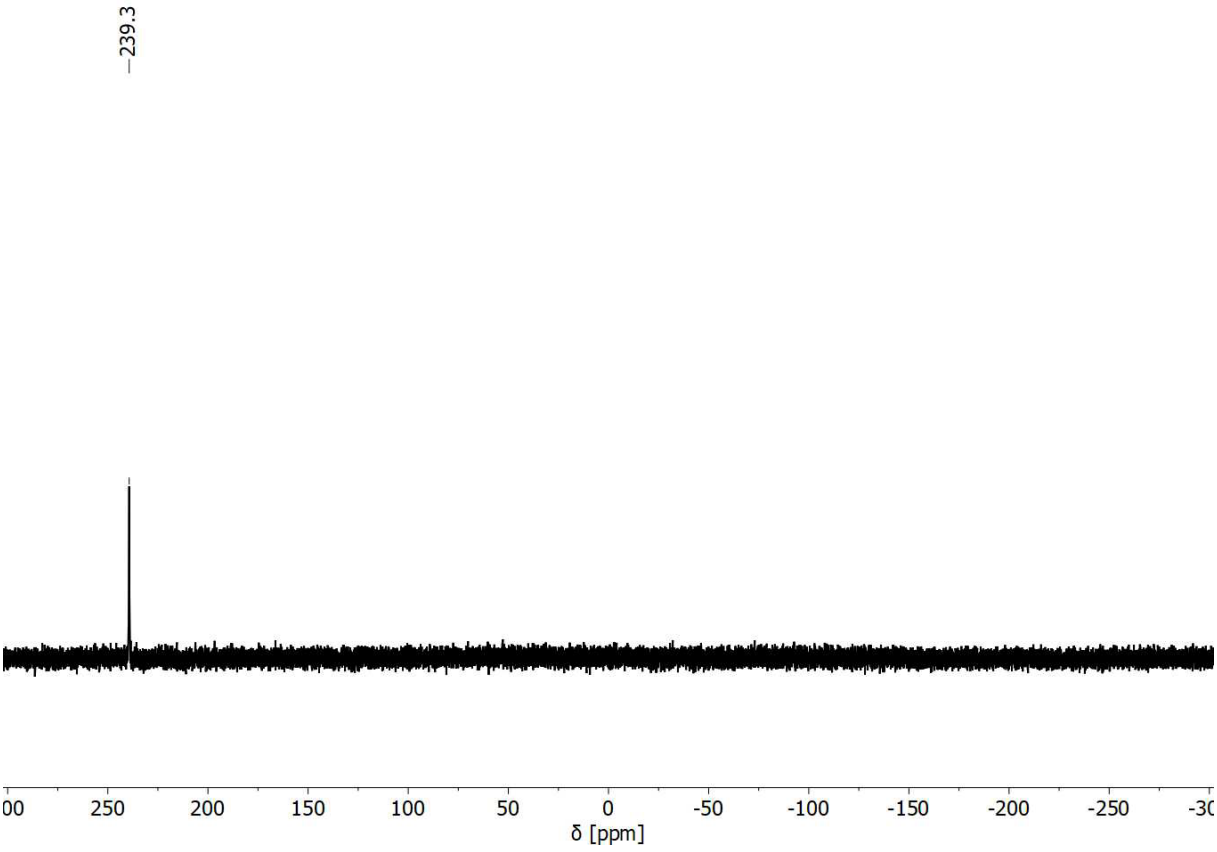


**Figure S10**: $^{31}P\{^{1}H\}$ NMR spectrum of **2a.**

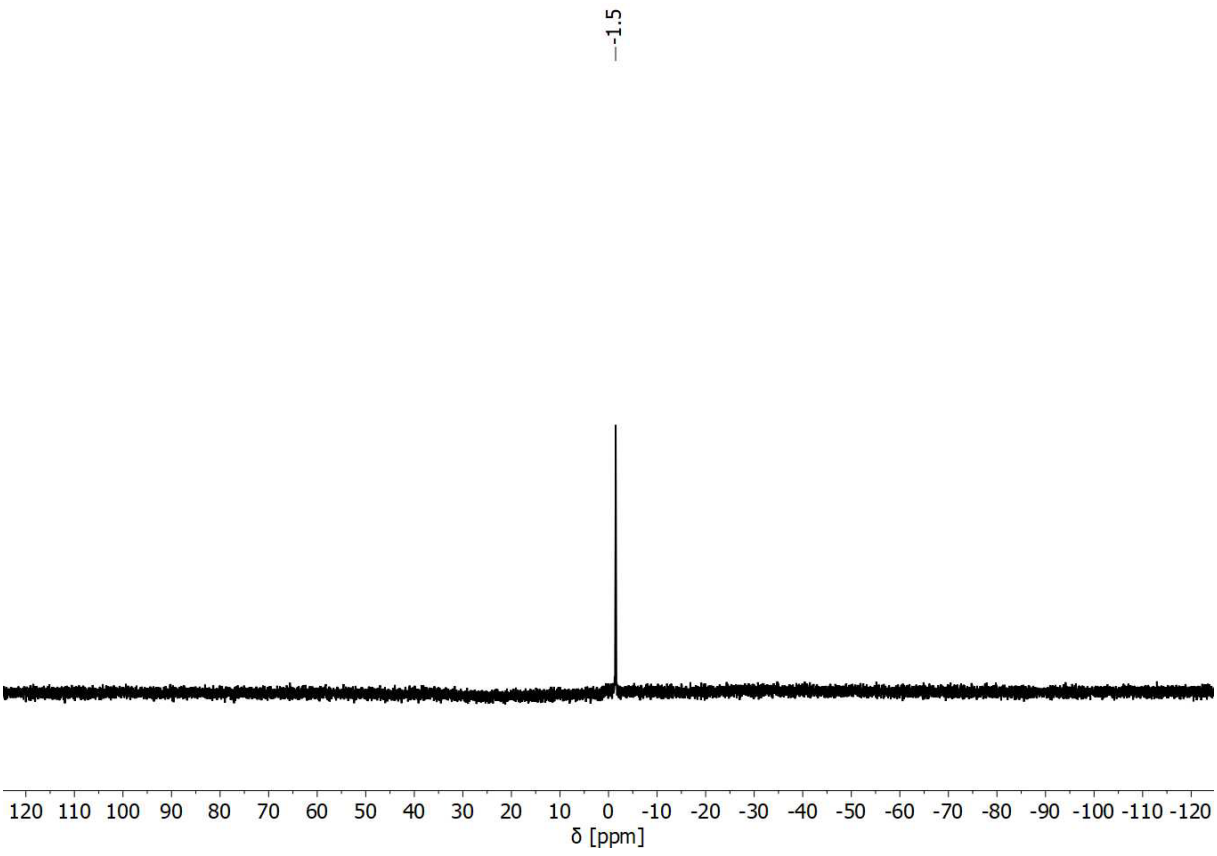


**Figure S11**: $^{11}B$ NMR spectrum of **2a.**

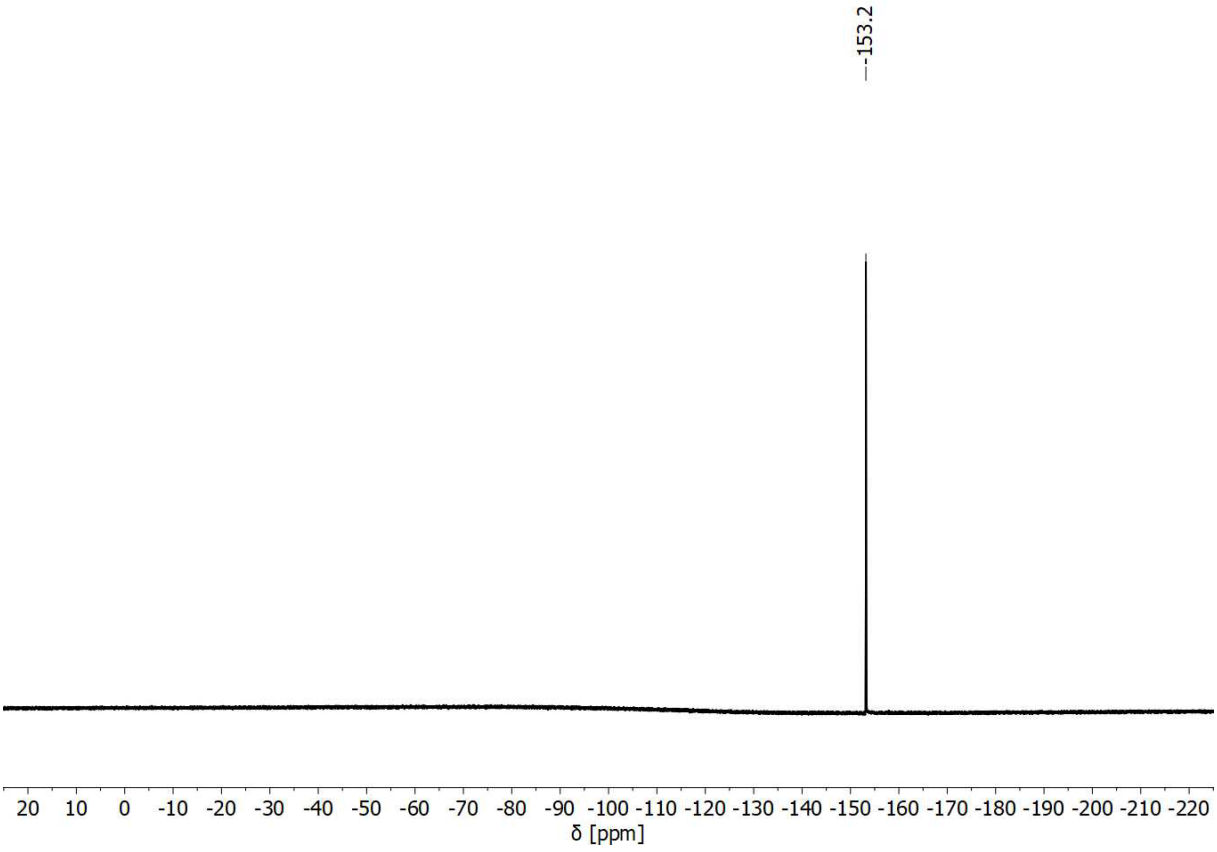


**Figure S12**: $^{19}F$ NMR spectrum of **2a.**

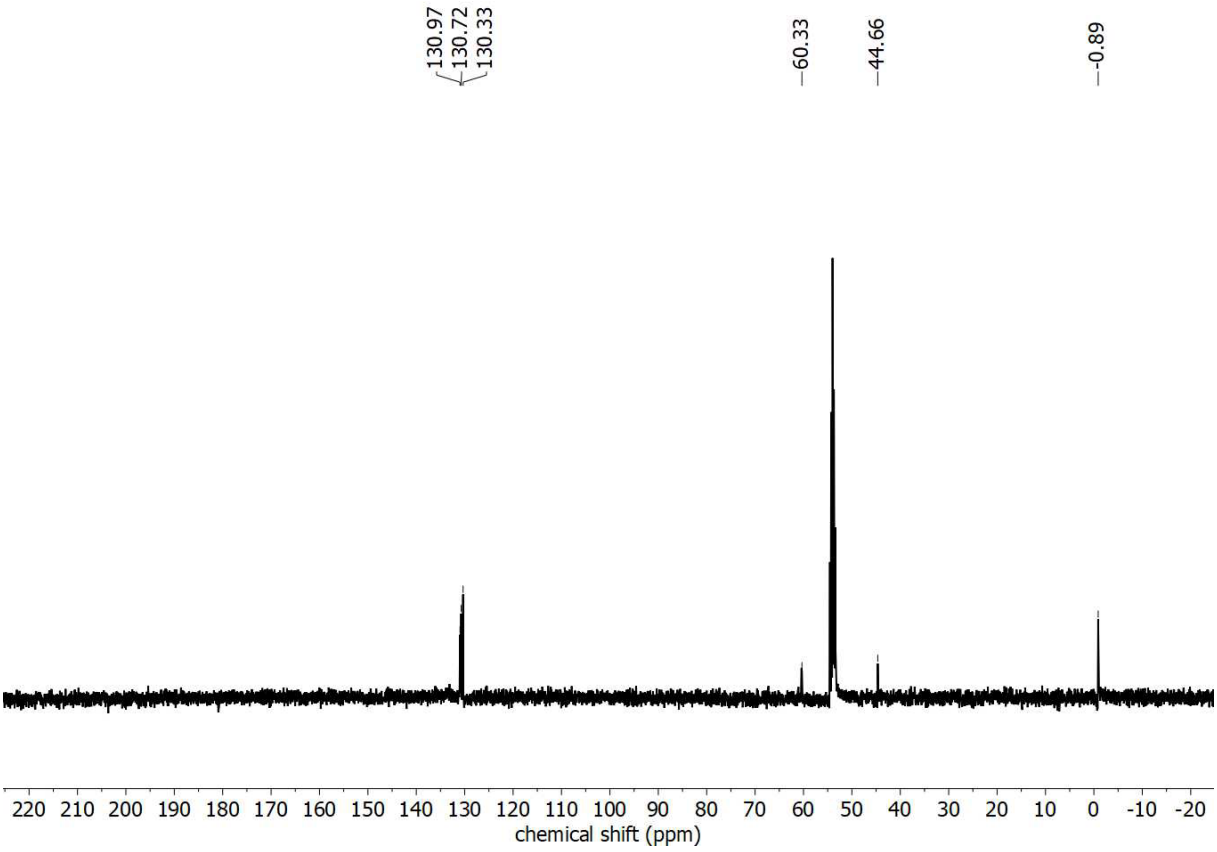


**Figure S13**: $^{13}C$ NMR spectrum of **2a.**

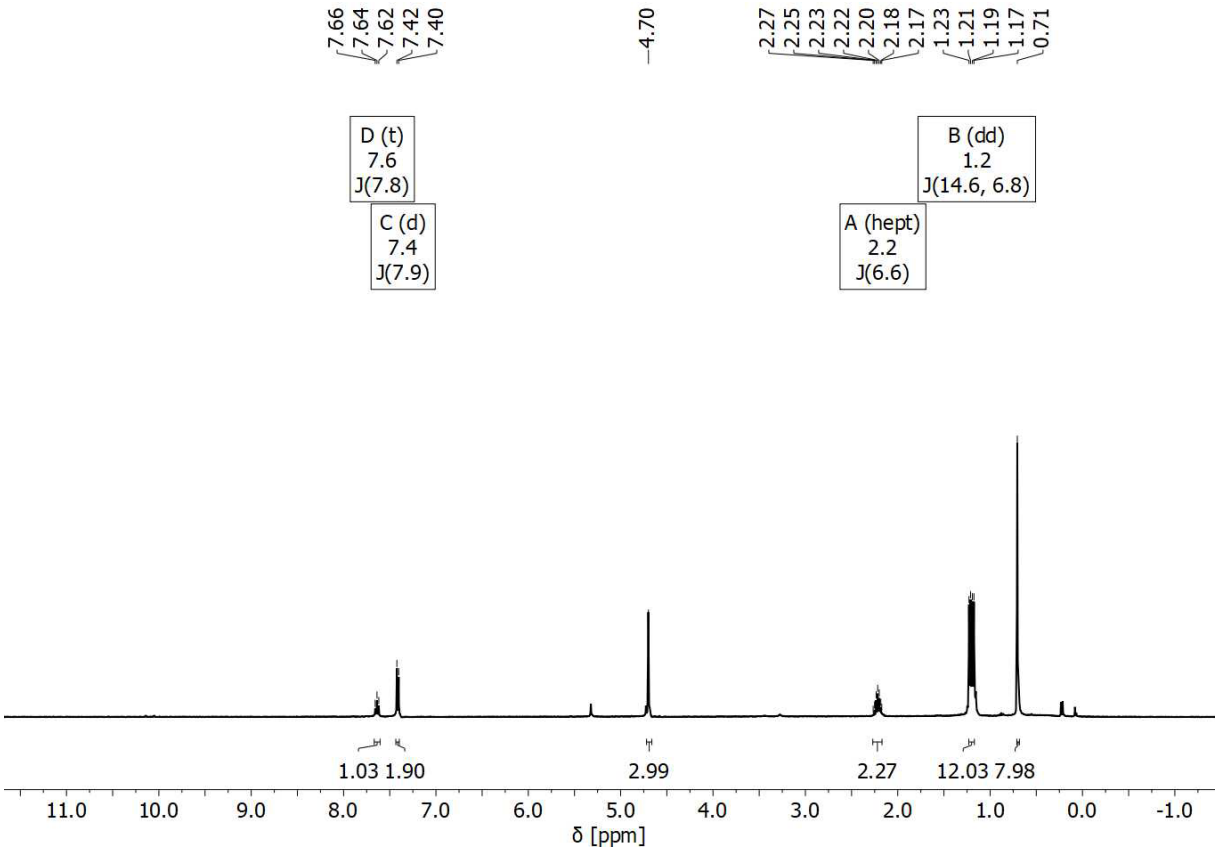


**Figure S14:** 1H NMR spectrum of **2b.**

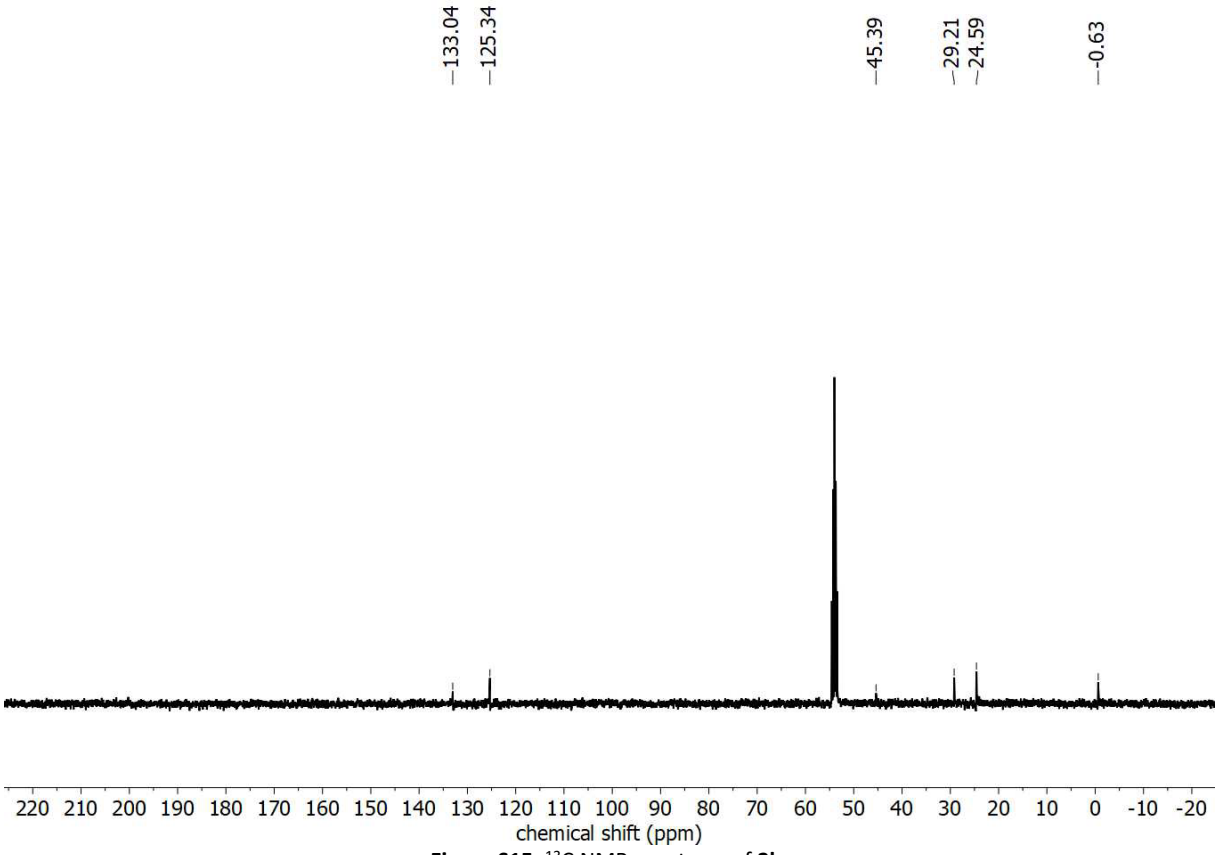


**Figure S15**: $^{13}C$ NMR spectrum of **2b.**

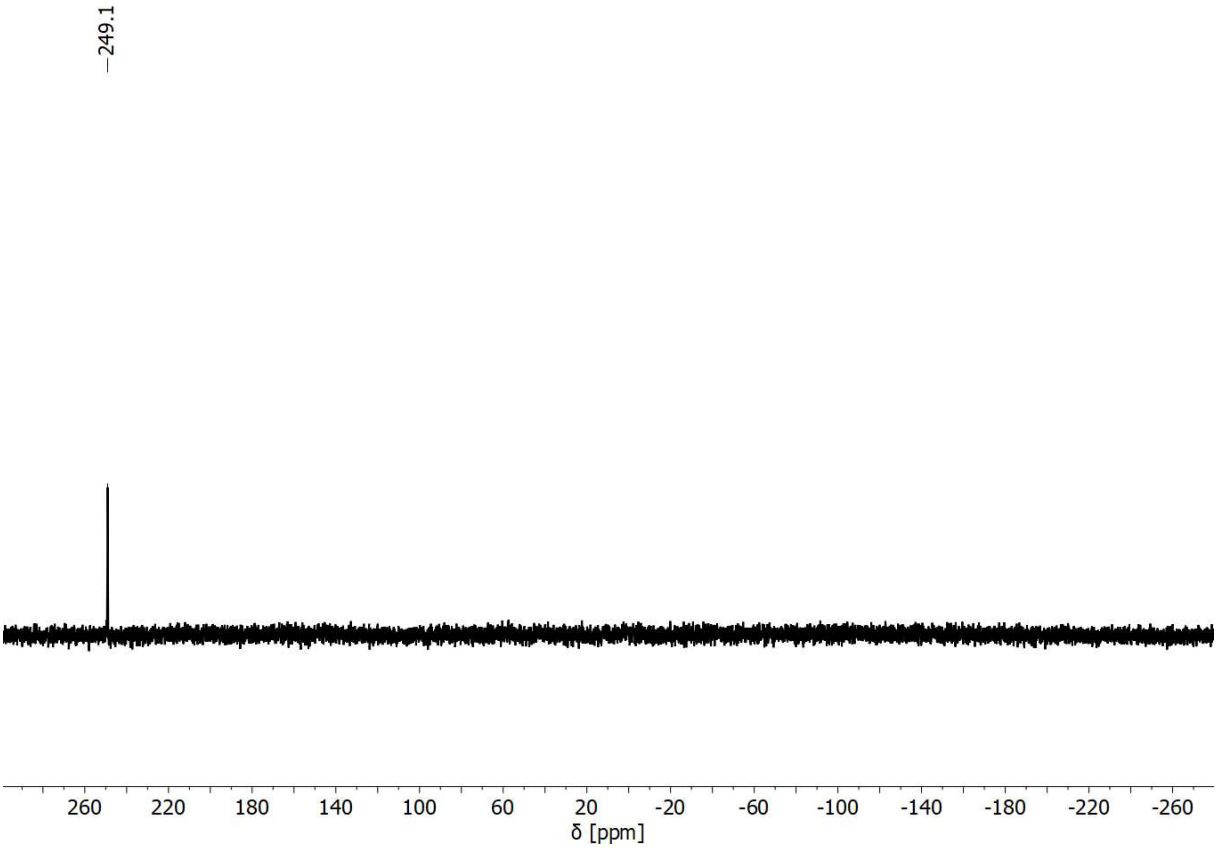


**Figure S16**: $^{31}P\{^{1}H\}$ NMR spectrum of **2b.**

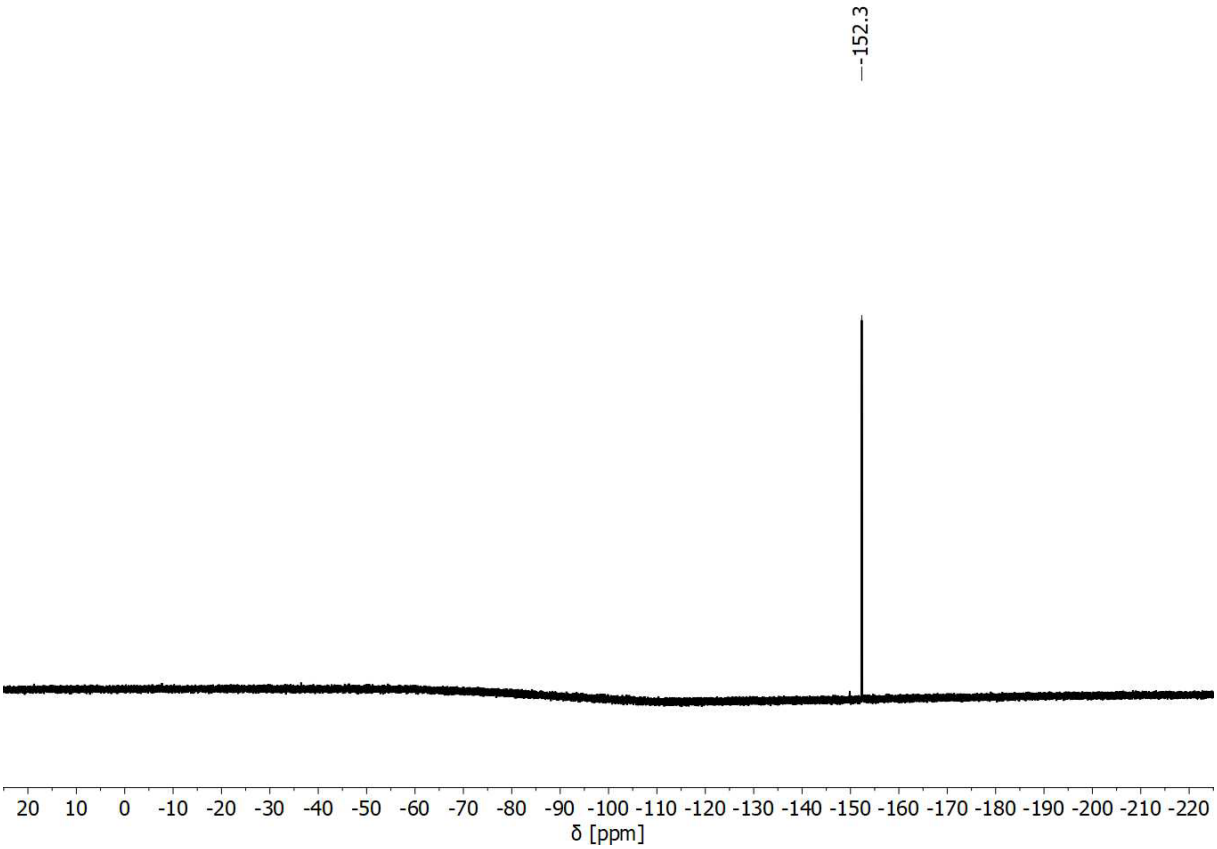


**Figure S17**: $^{19}F$ NMR spectrum of **2b.**

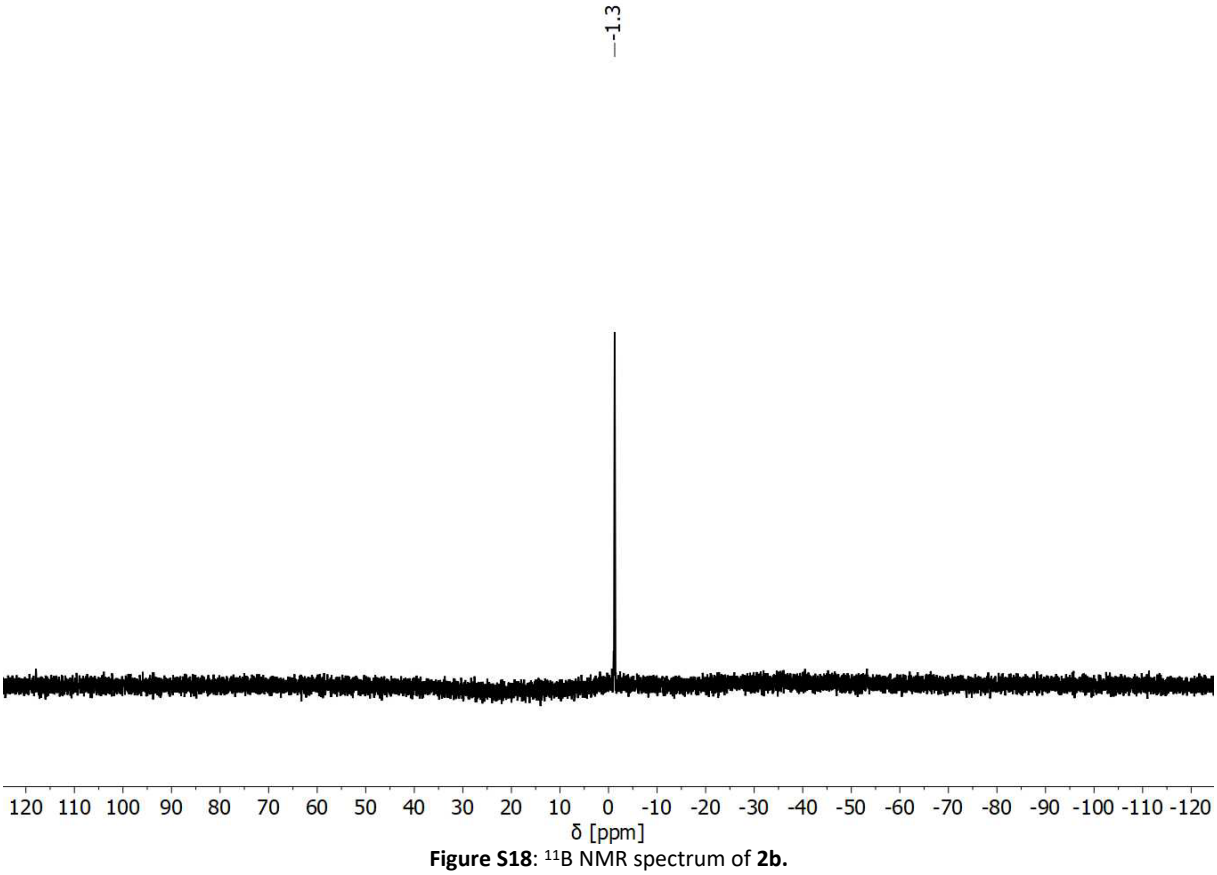


**Figure S18**: $^{11}B$ NMR spectrum of **2b.**

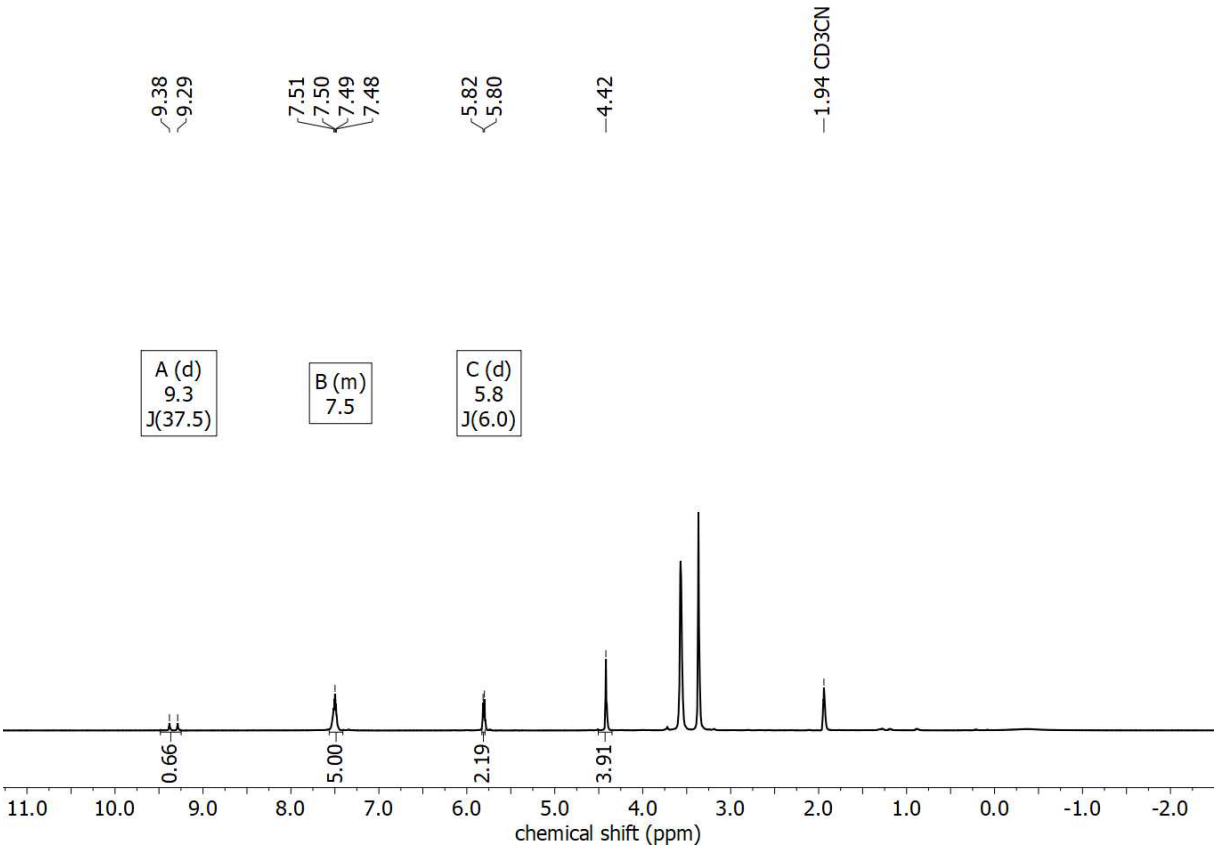


**Figure S19:** 1H NMR spectrum of **3a.**

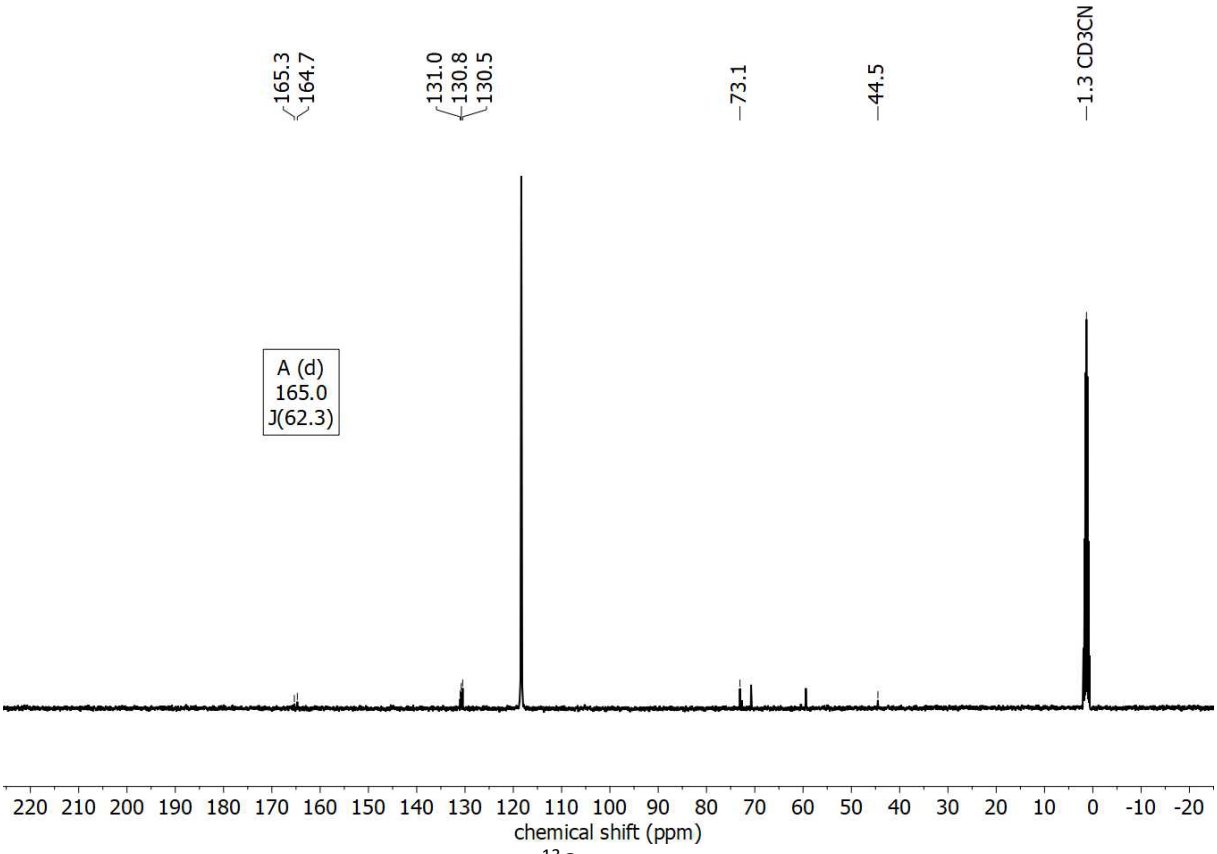


**Figure S20**: $^{13}C$ NMR spectrum of **3a.**

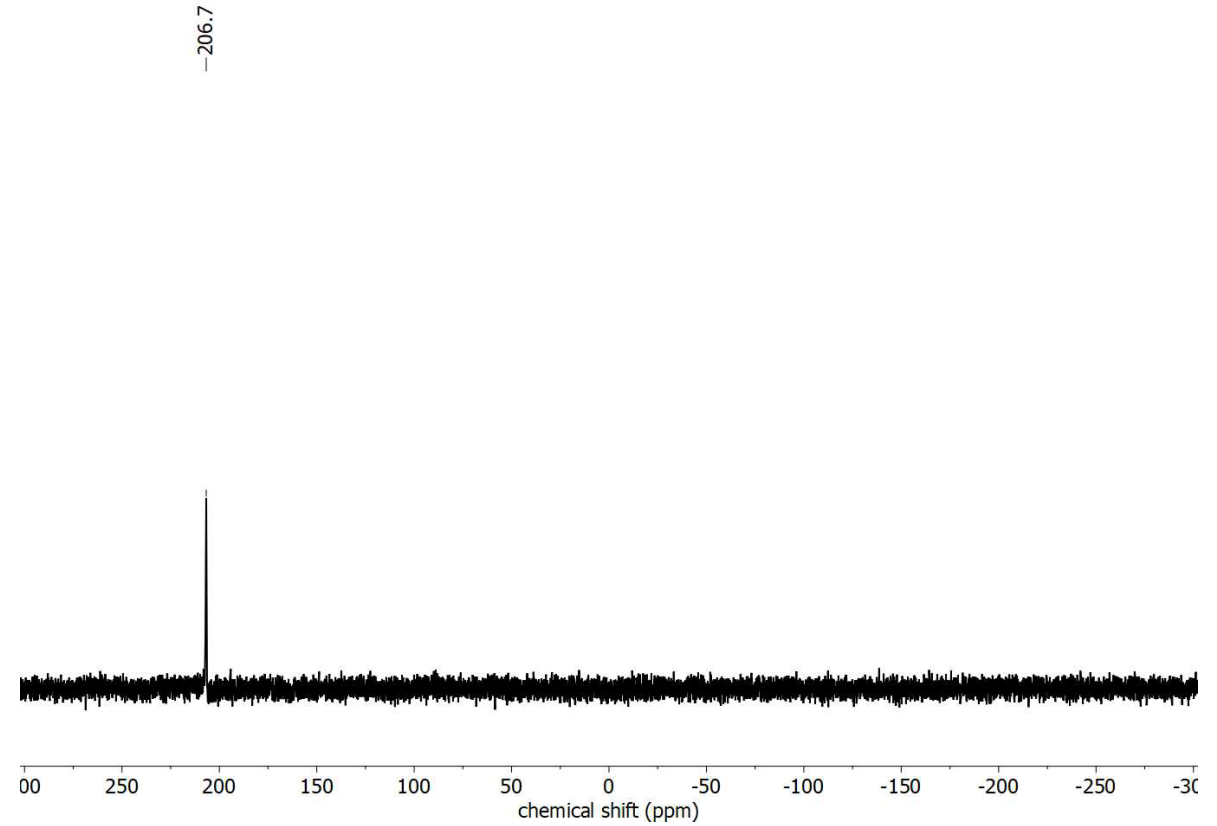


**Figure S21**: $^{31}P\{^{1}H\}$ NMR spectrum of **3a.**

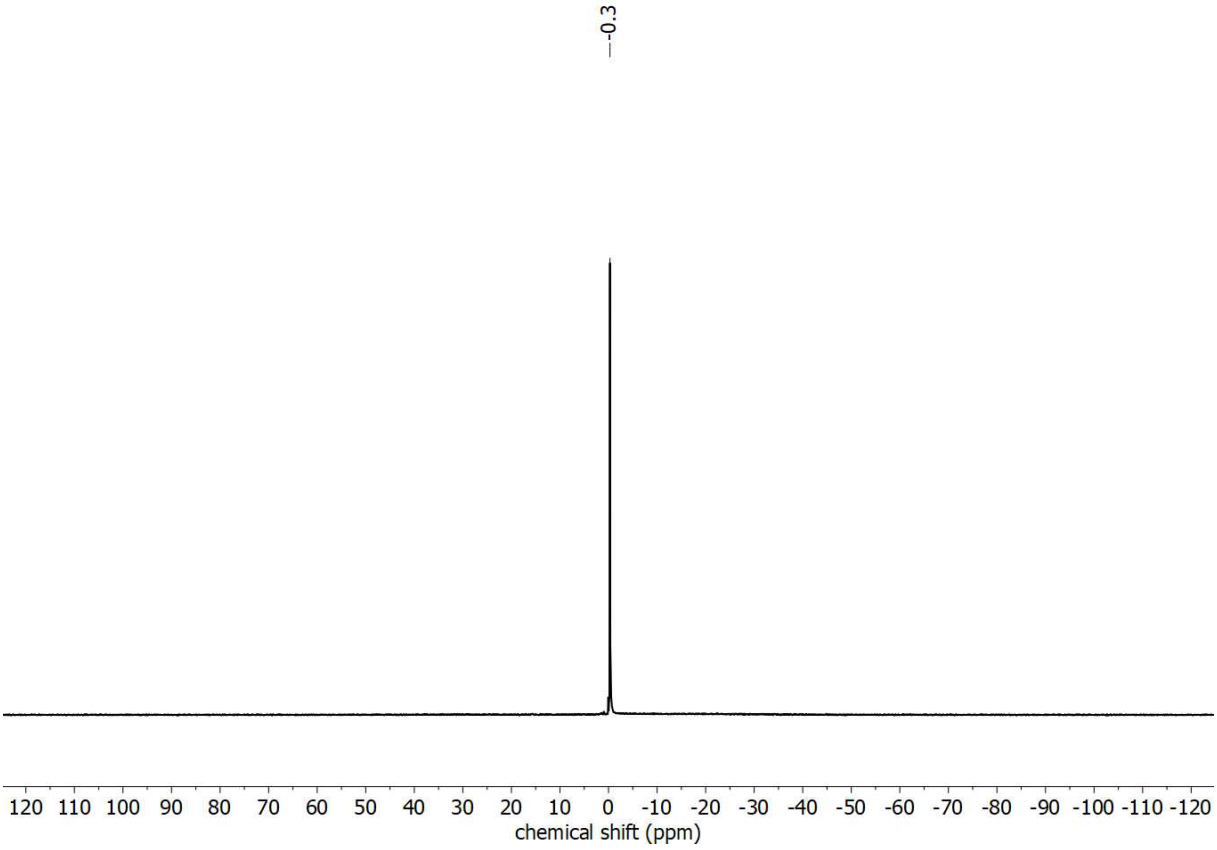


**Figure S22**: $^{11}B$ NMR spectrum of **3a.**

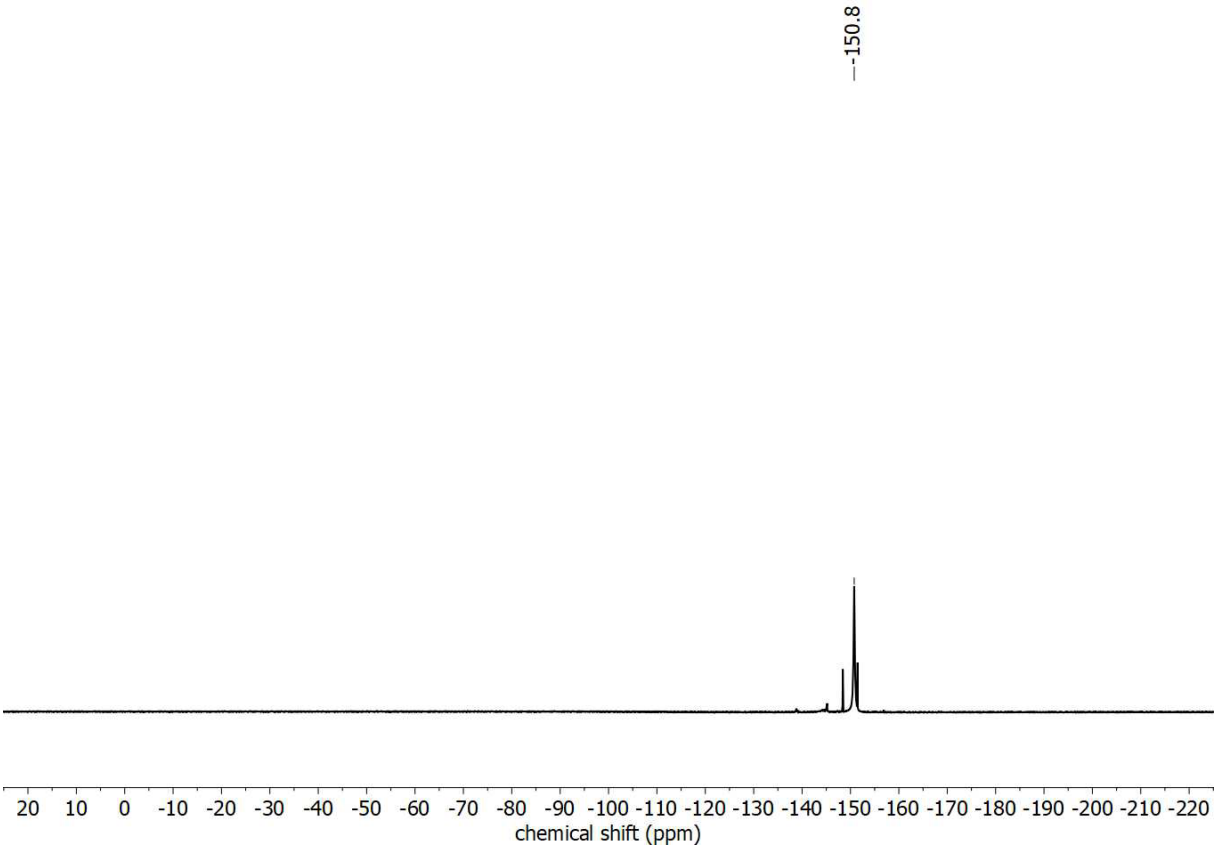


**Figure S23**: $^{19}F$ NMR spectrum of **3a.**

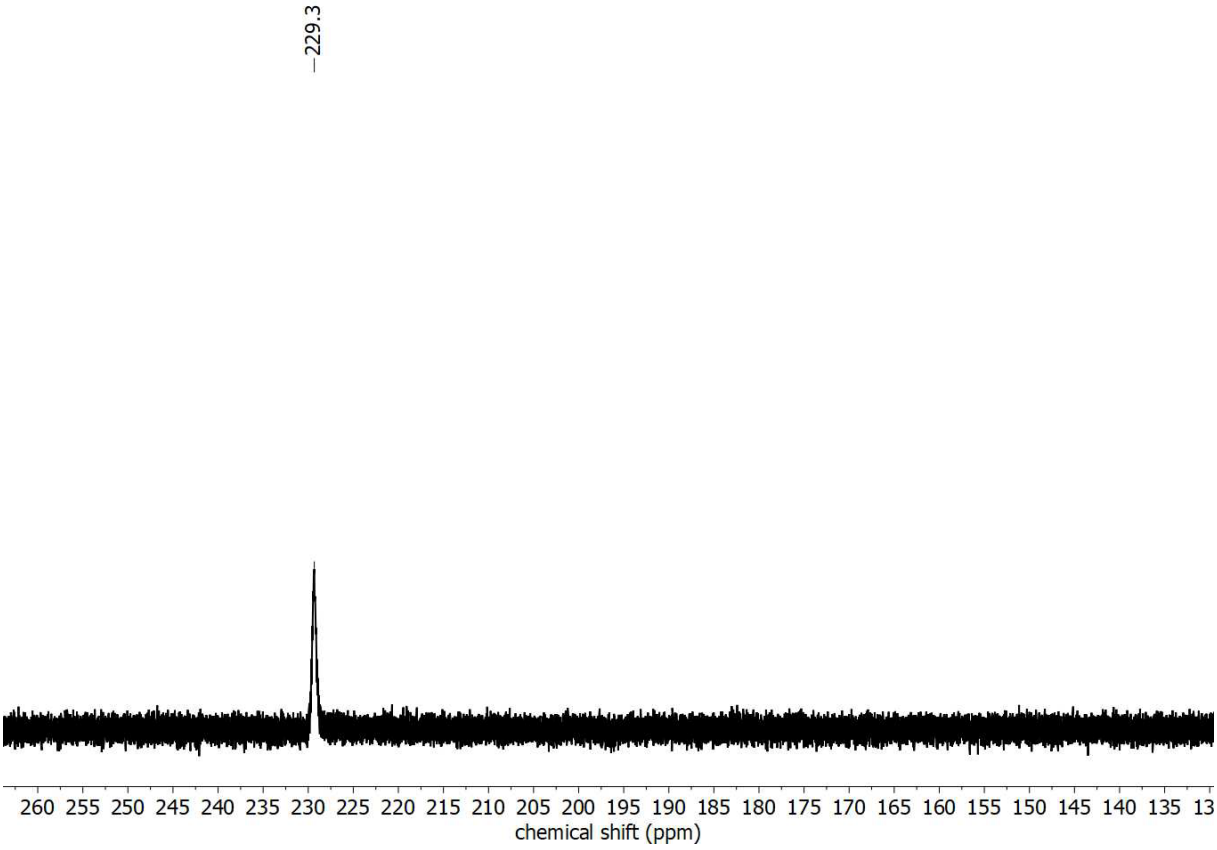


**Figure S24**: $^{31}P\{^{1}H\}$ NMR spectrum of **4a.**

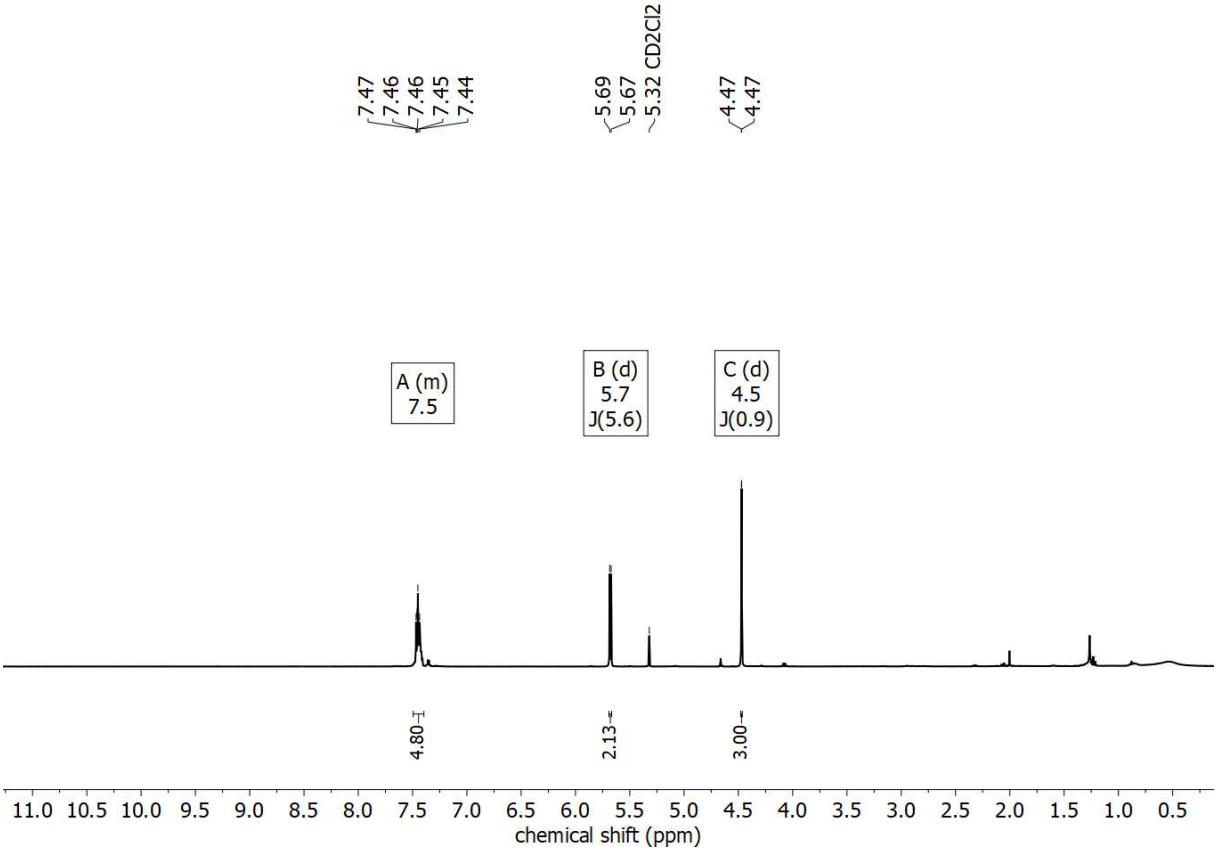


**Figure S25:** 1H NMR spectrum of **4a.**

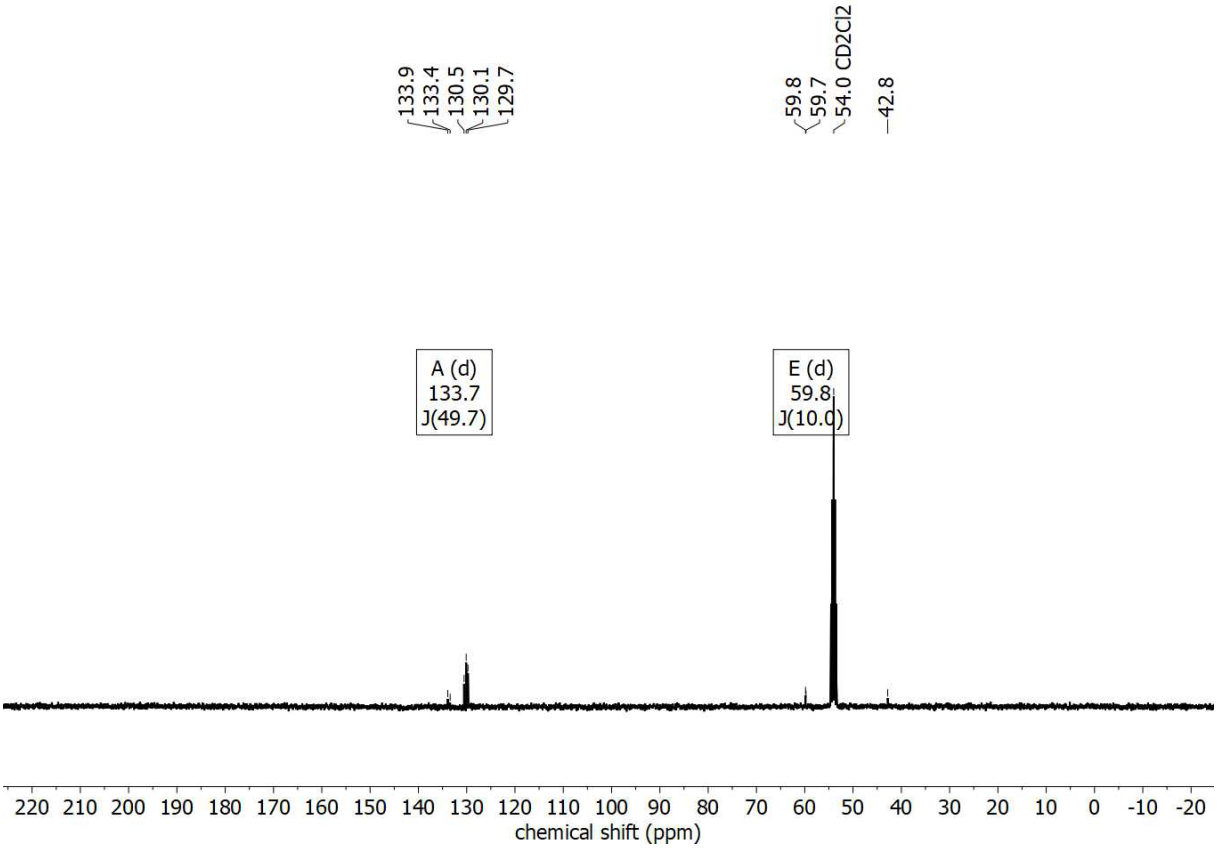


**Figure S26**: $^{13}C$ NMR spectrum of **4a.**

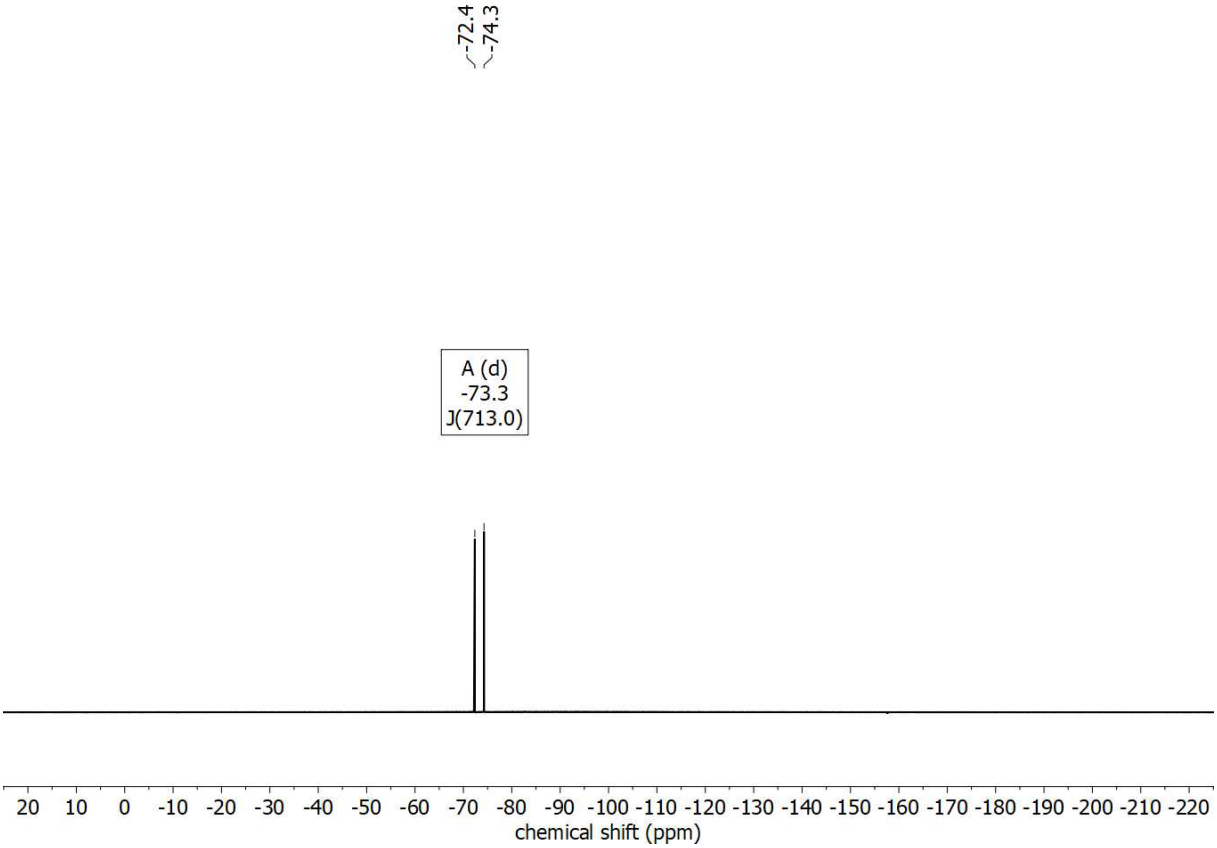


**Figure S27**: $^{19}F$ NMR spectrum of **5a.**

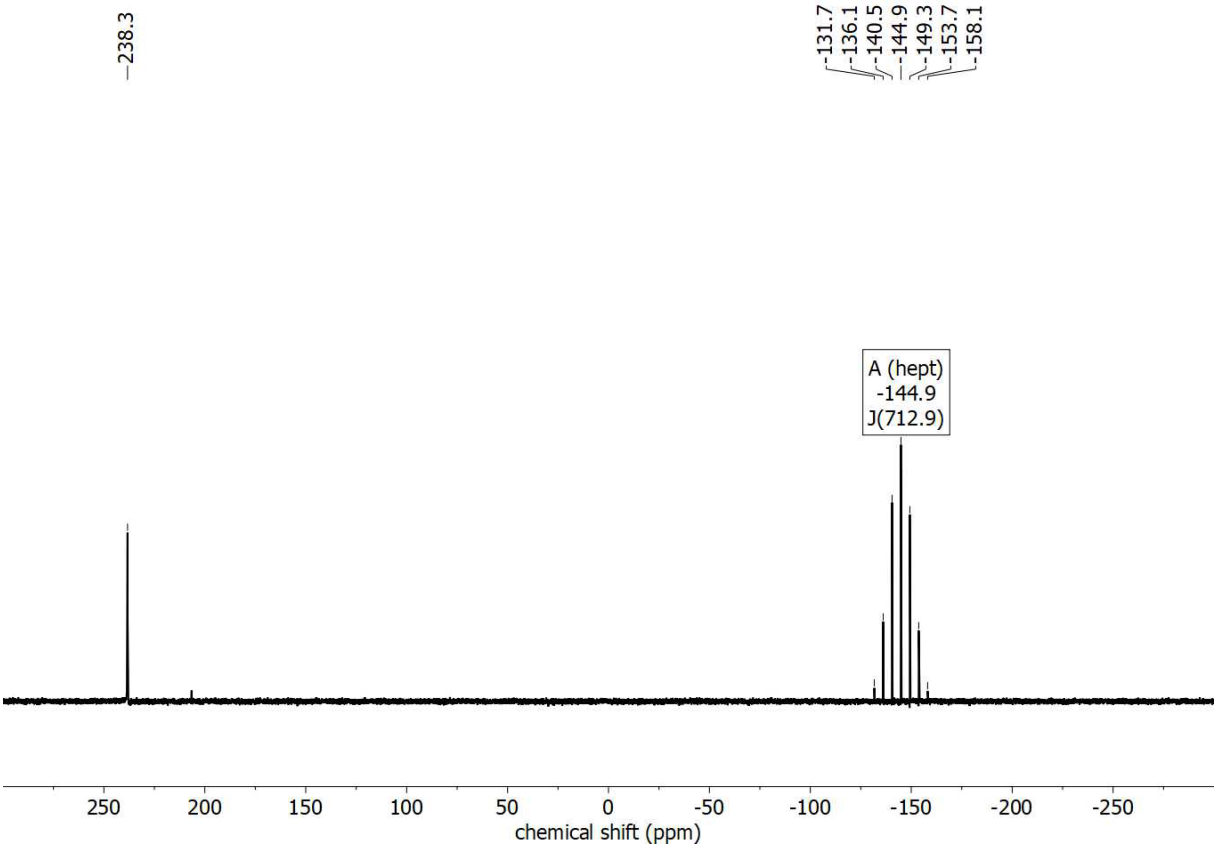


**Figure S28**: $^{31}P\{^{1}H\}$ NMR spectrum of **5a.**

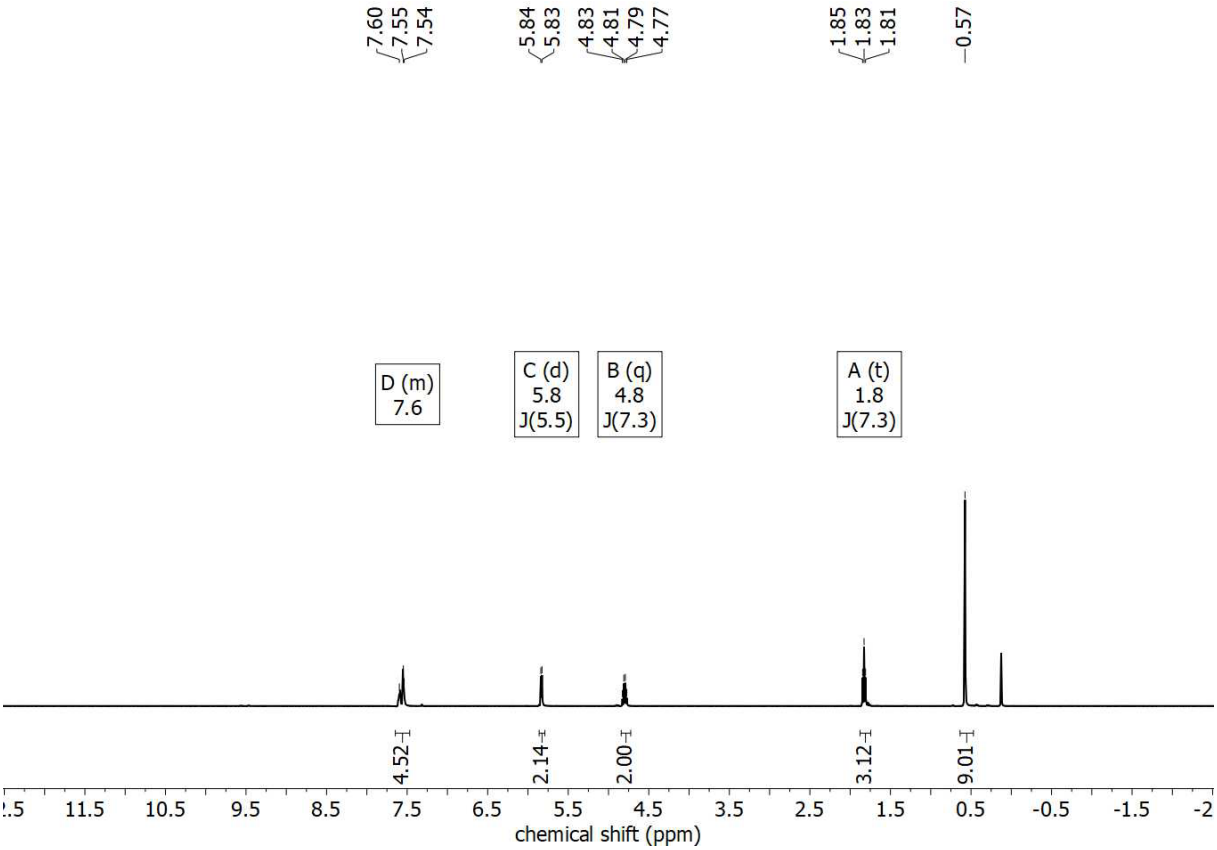


**Figure S29:** 1H NMR spectrum of **5a.**

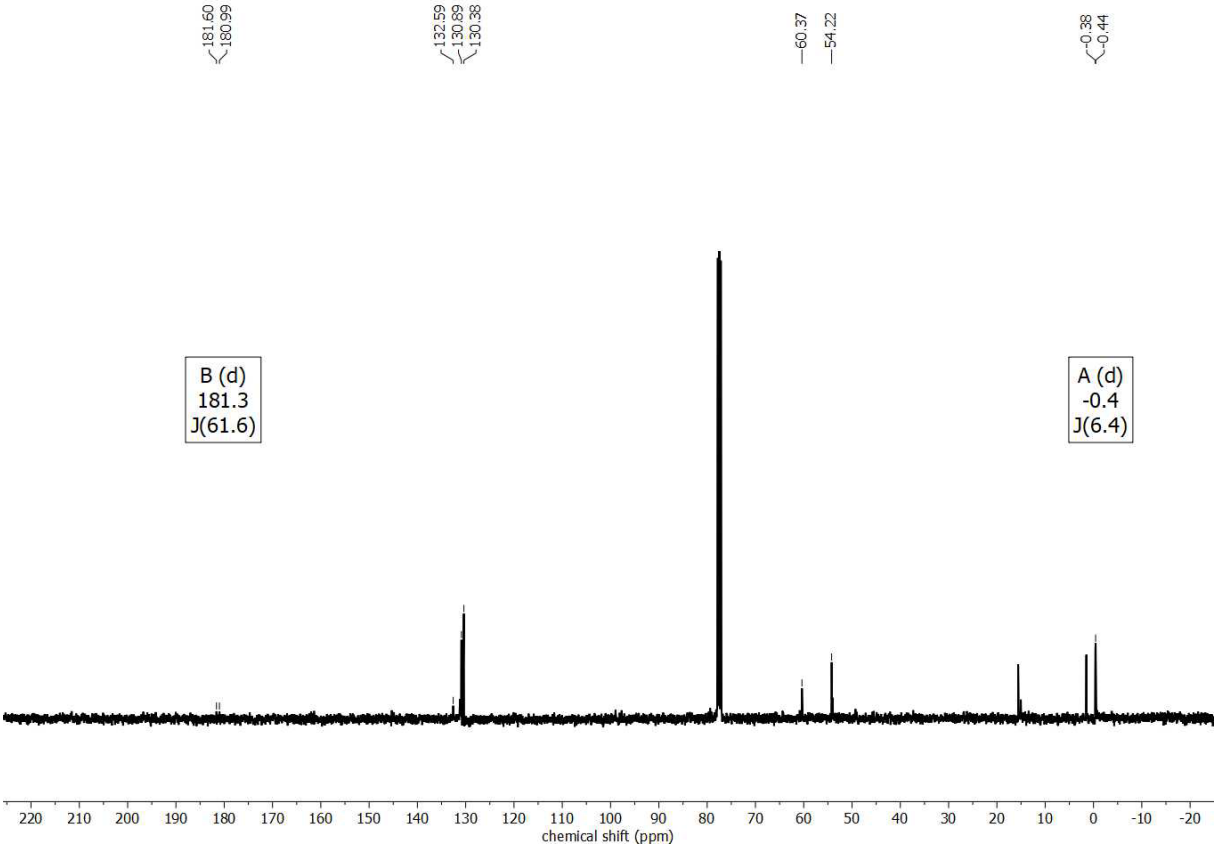


**Figure S30**: $^{13}C$ NMR spectrum of **5a.**

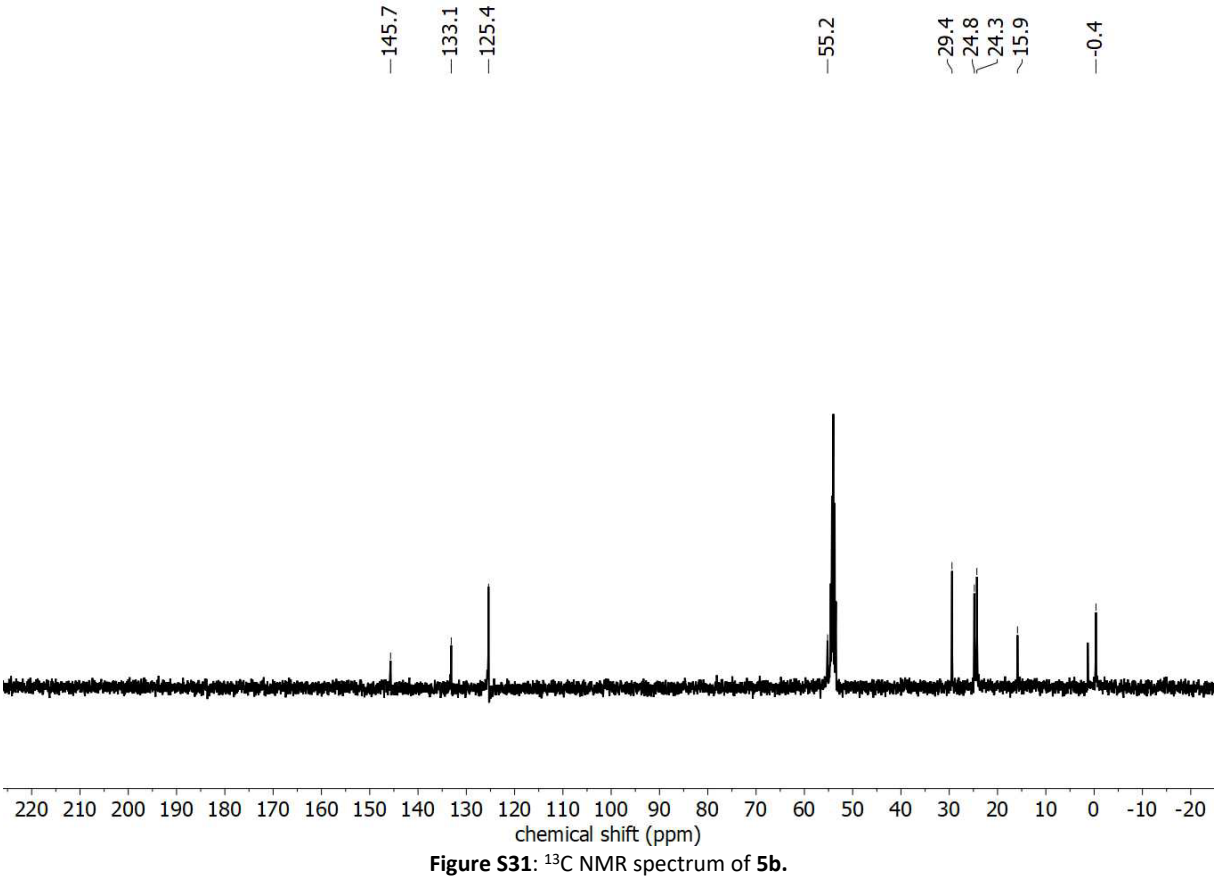


**Figure S31**: $^{13}C$ NMR spectrum of **5b.**

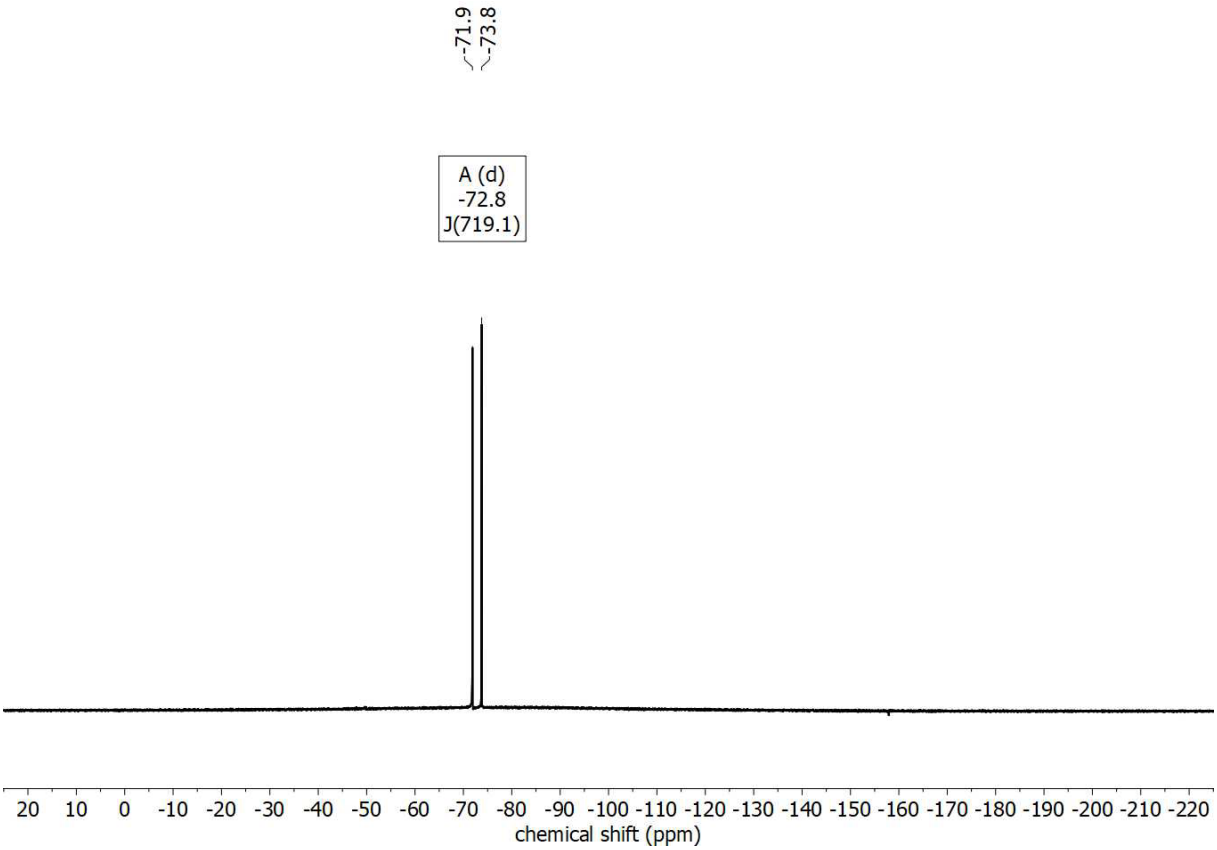


**Figure S32**: $^{19}F$ NMR spectrum of **5b.**

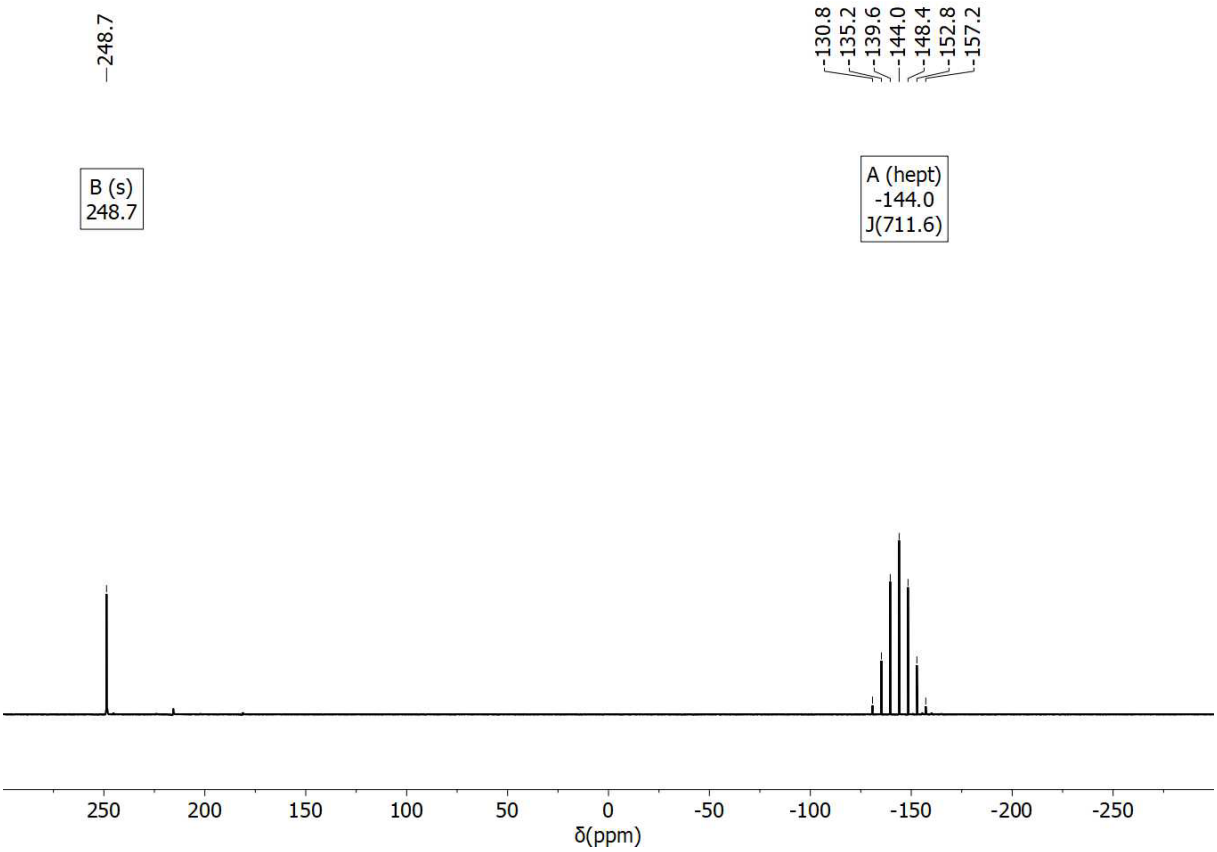


**Figure S33**: $^{31}P\{^{1}H\}$ NMR spectrum of **5b.**

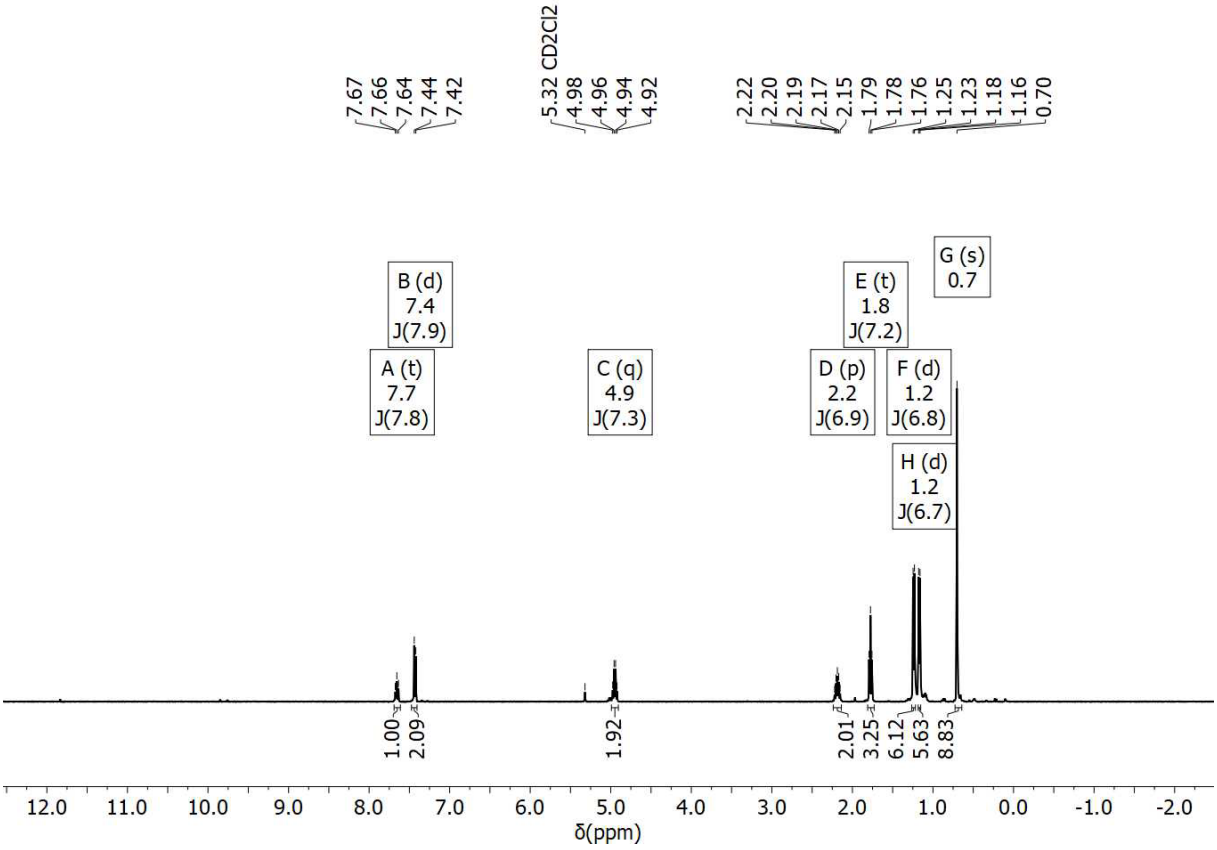


**Figure S34:** 1H NMR spectrum of **5b.**

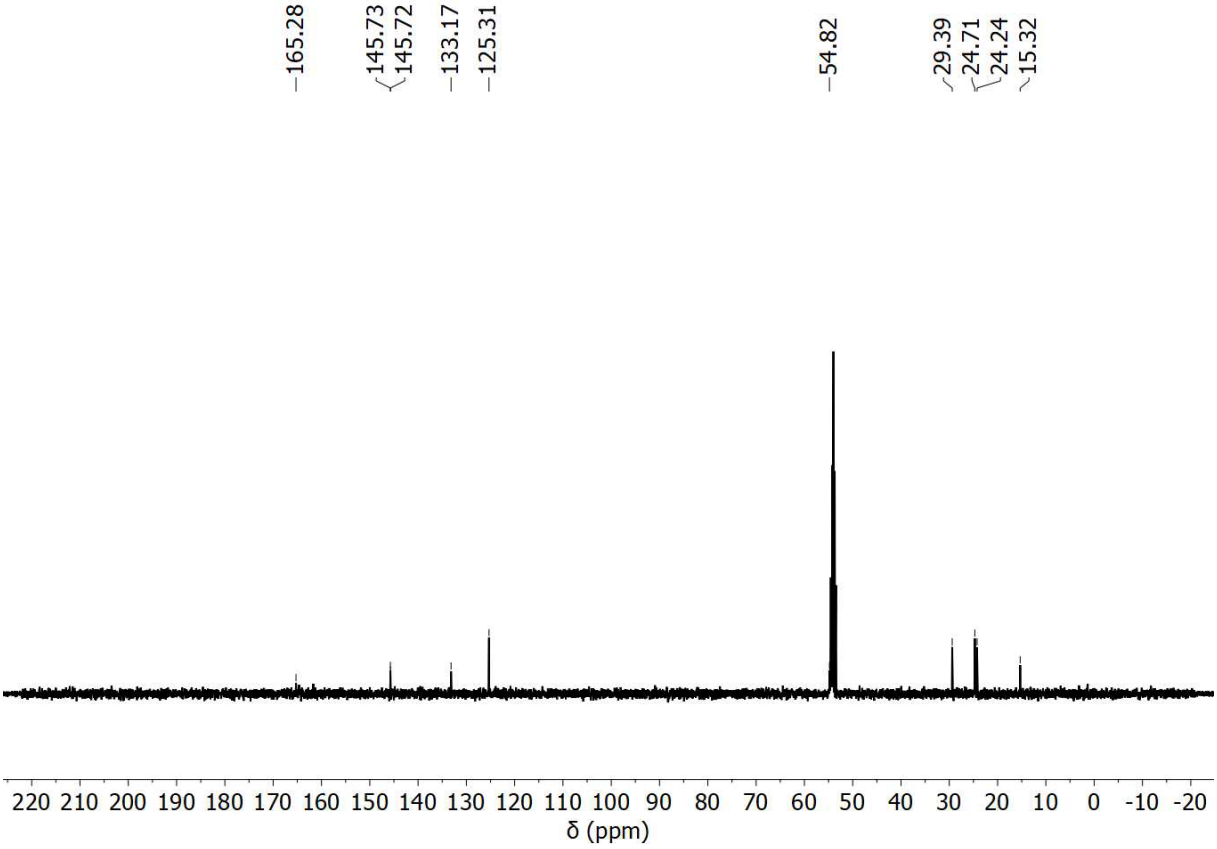


**Figure S35**: $^{13}C$ NMR spectrum of **6b.**

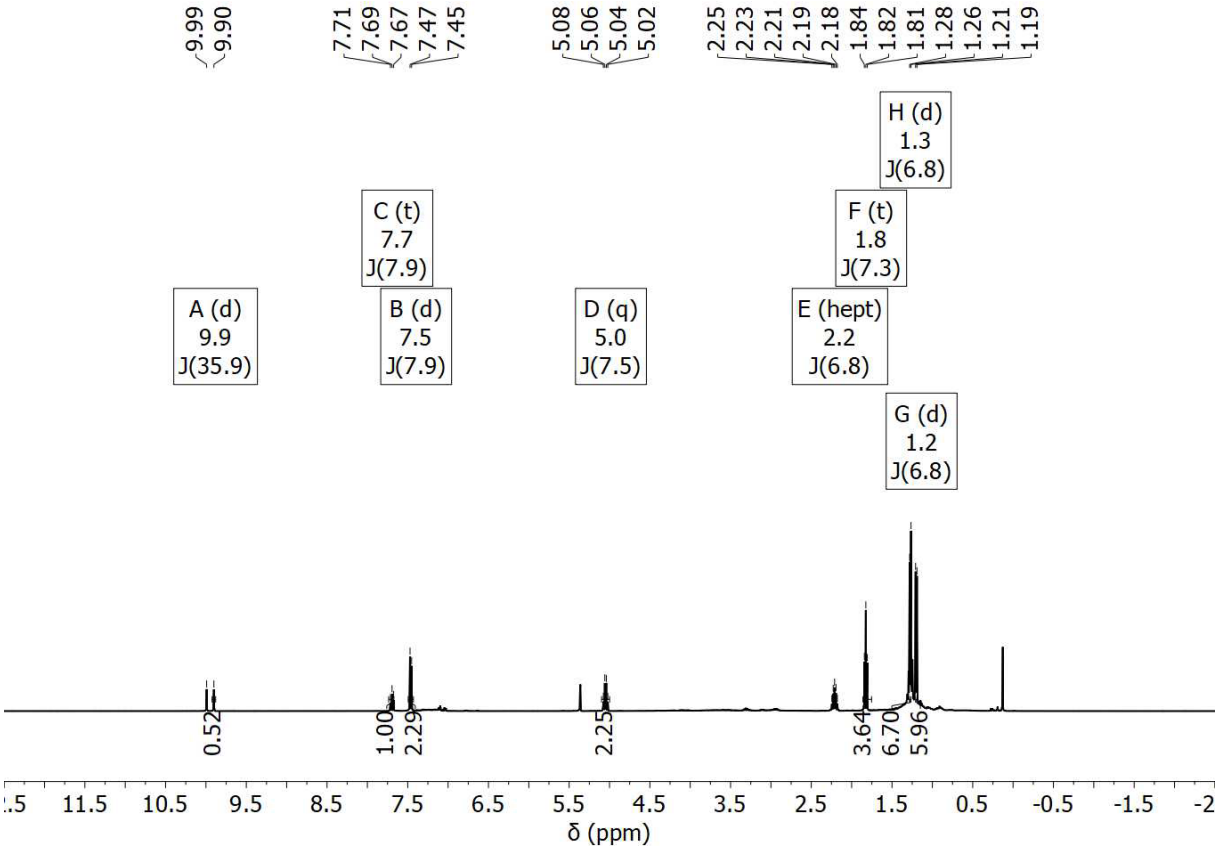


**Figure S36:** 1H NMR spectrum of **6b.**

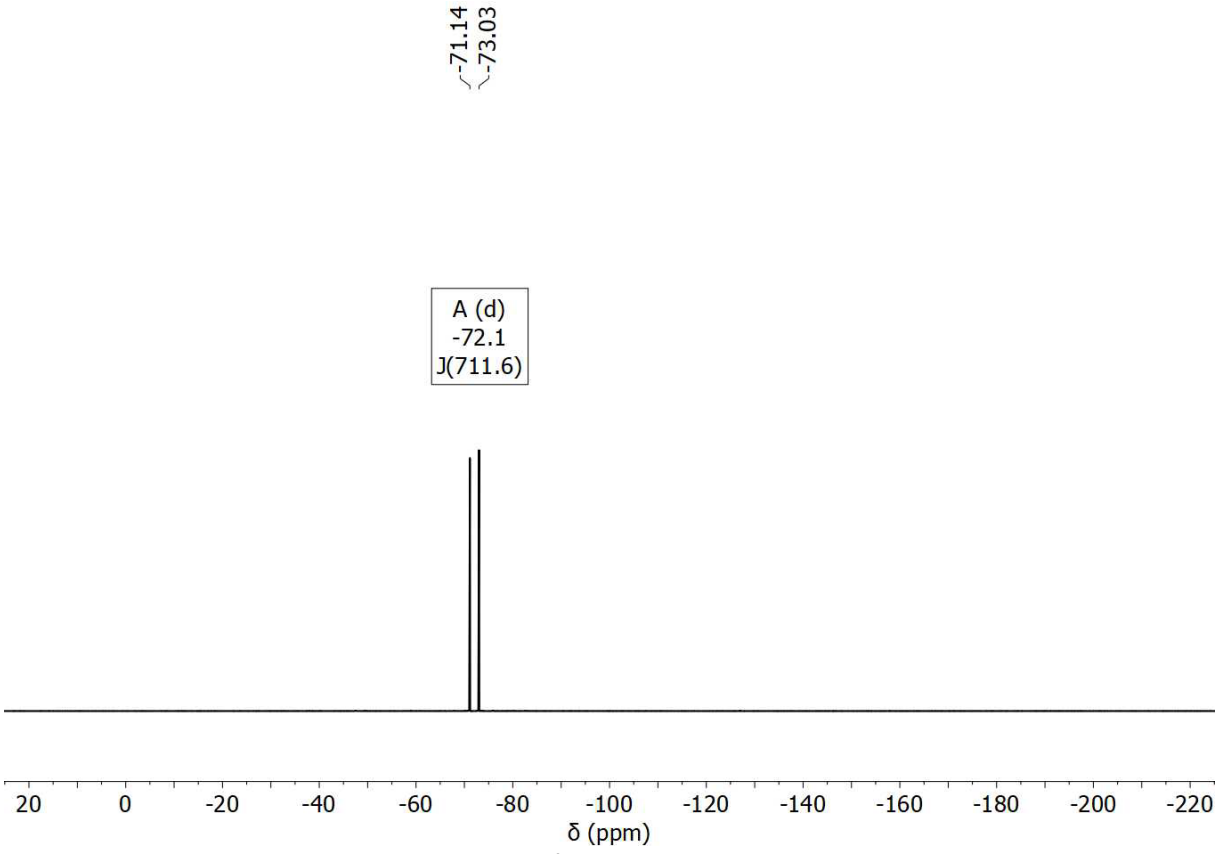


**Figure S37**: $^{19}F$ NMR spectrum of **6b.**

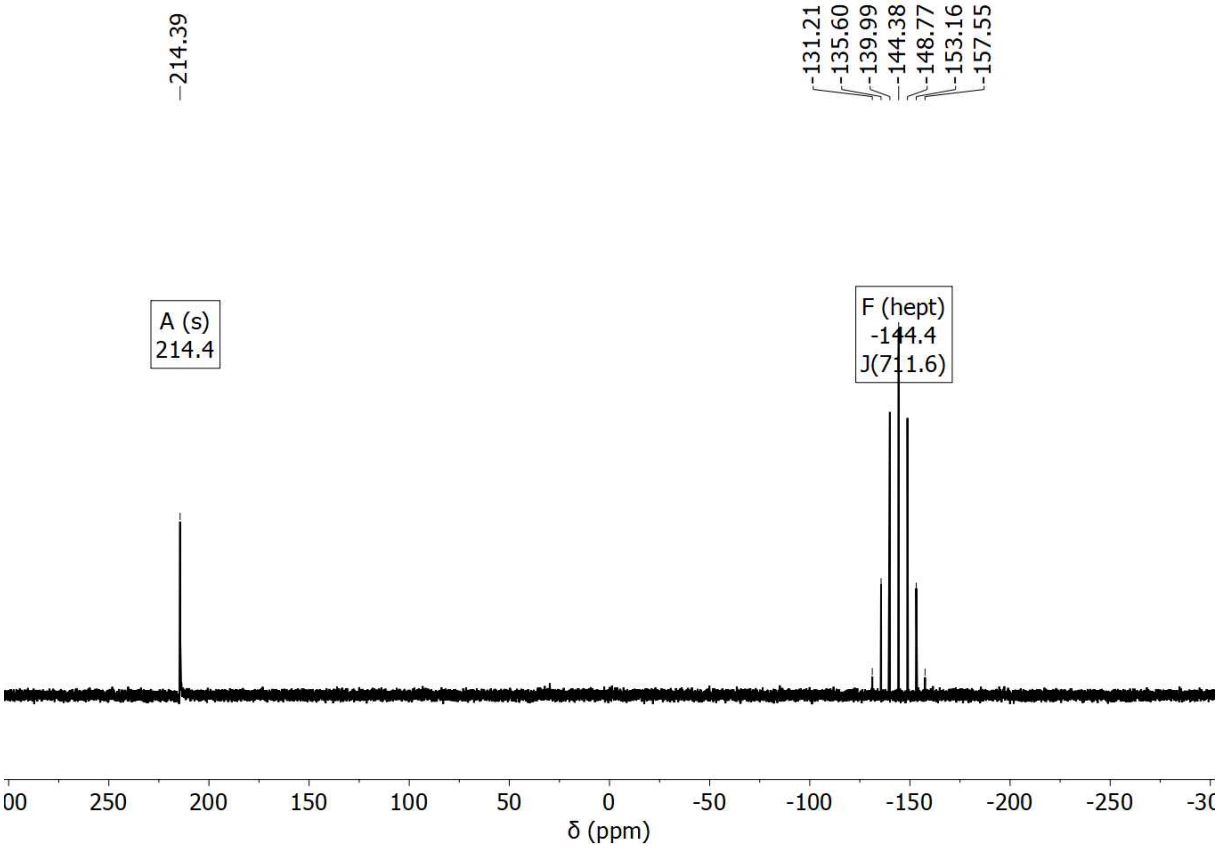


**Figure S38**: $^{31}P\{^{1}H\}$ NMR spectrum of **6b**

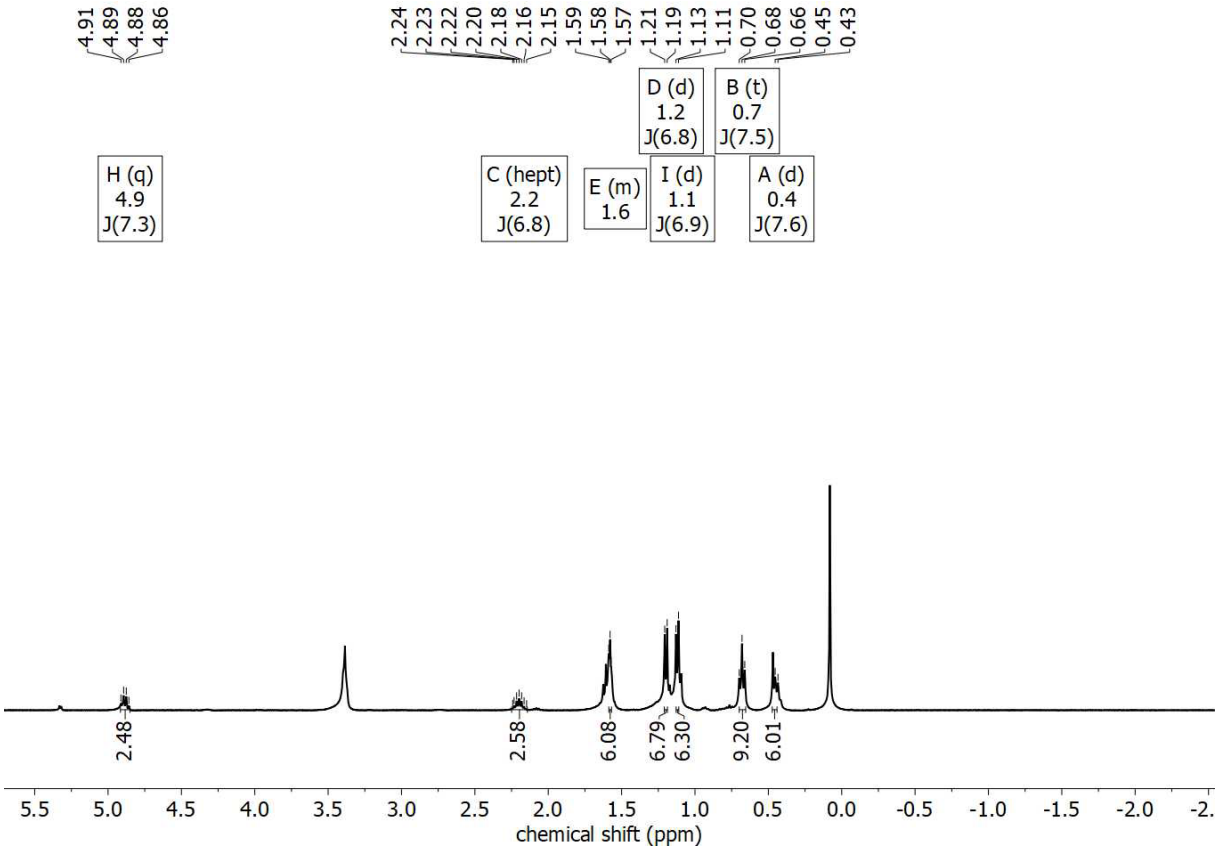


**Figure S39:** $^{1}H$ NMR spectrum of **7b.**

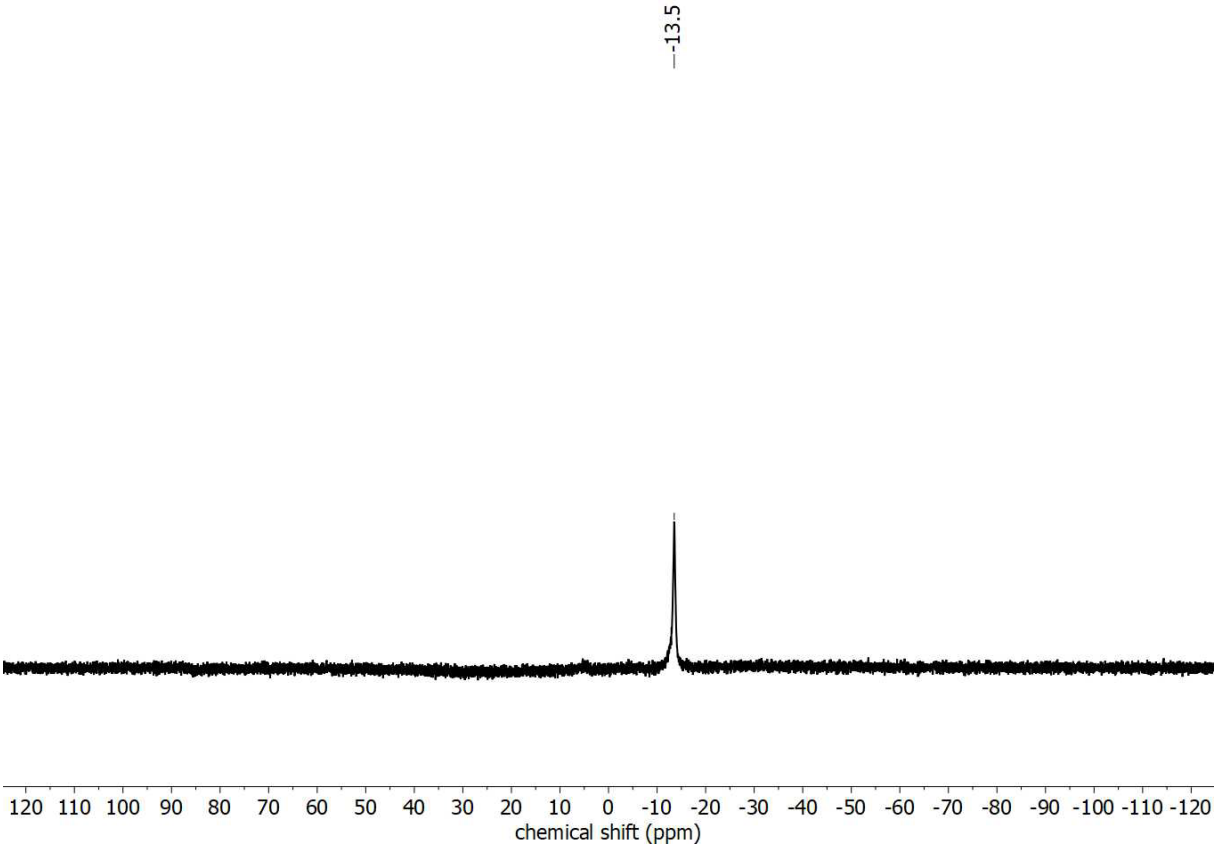


**Figure S40**: $^{11}B$ NMR spectrum of **7b.**

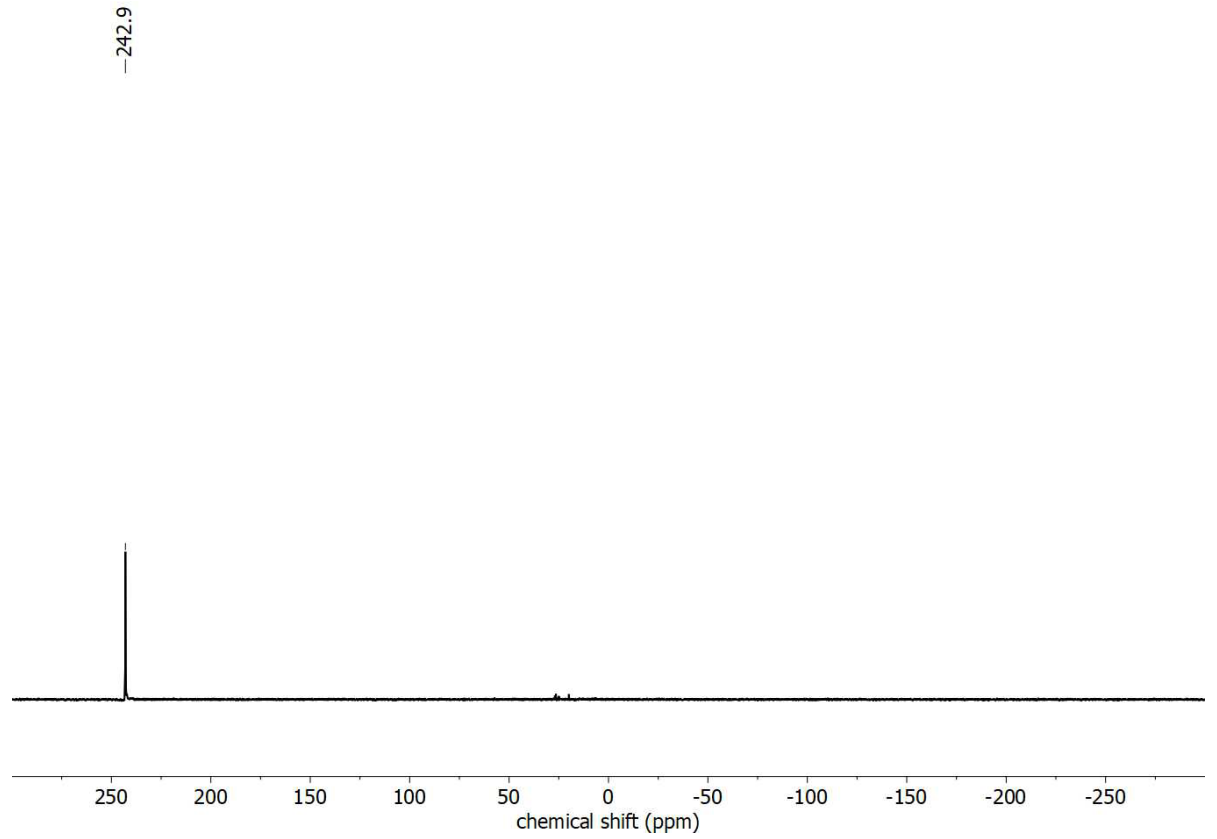


**Figure S41**: $^{31}P\{^{1}H\}$ NMR spectrum of **7b.**

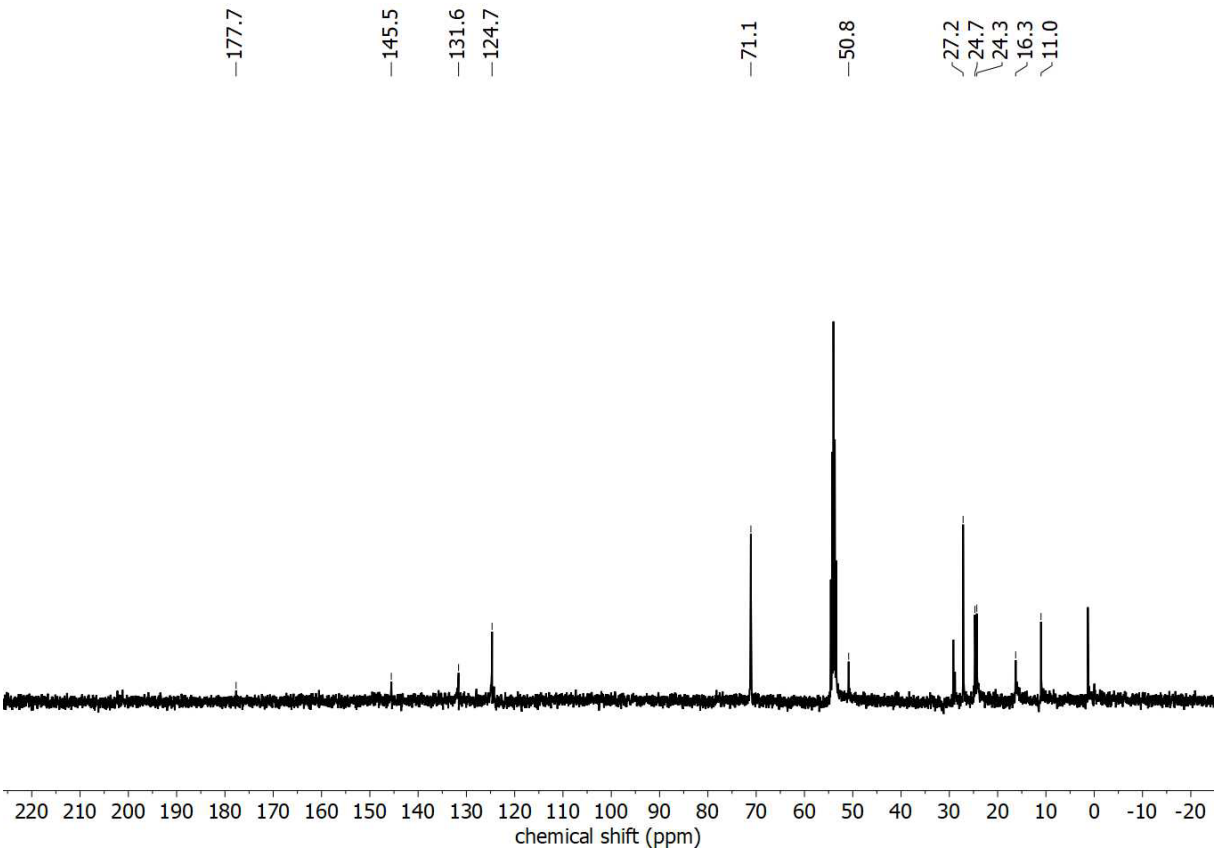


**Figure S42**: $^{13}C$ NMR spectrum of **7b.**

## 5. DFT Calculations

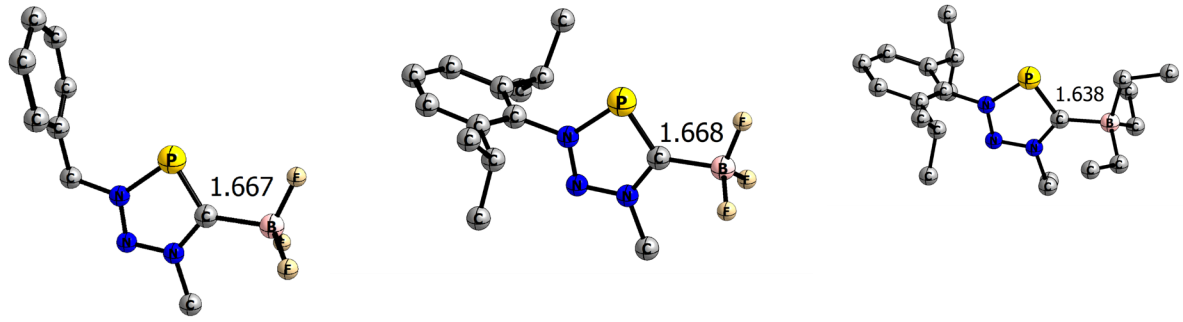


**4a** **4b** **7b**

**Figure S43.** Optimized structures at the B3LYP-D3(BJ)/def2-TZVP level of theory. Hydrogen atoms are omitted for clarity.

**Table S6**. NBO results calculated at B3LYP-D3(BJ)/def2-TZVPP level of theory: partial charges, Q (in e), Wiberg bond order, WBI (in a.u.).

| | **4a** | **4b** | **7b** |
|---|---|---|---|
| **Q($C_{carb}$)** | -0.41 | -0.41 | -0.23 |
| **Q(P)** | +0.81 | 0.81 | +0.78 |
| **Q(PHC)** | +0.47 | +0.46 | +0.51 |
| **Q($BR_3$)** | -0.47 | -0.46 | -0.51 |
| **WBI(C−B)** | 0.71 | 0.71 | 0.87 |

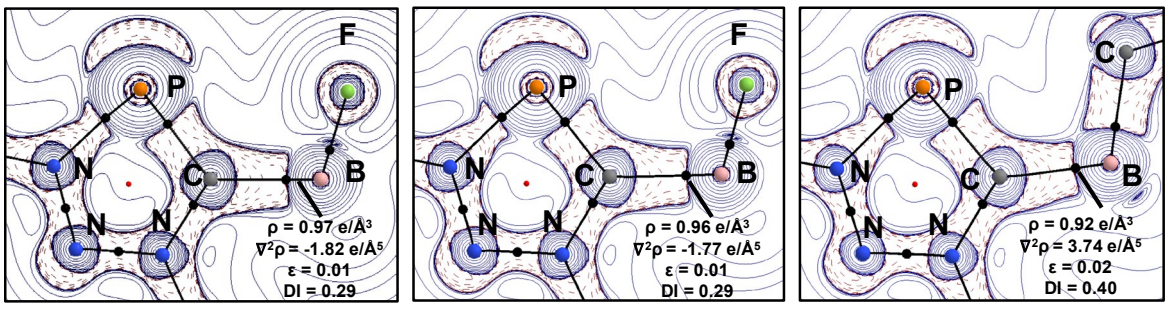


**4a** **4b** **7b**

**Figure S44**. Laplacian distribution of the electron density of compounds **4a/b** and **7b** (B3LYP-D3(BJ)/def2-TZVP//B3LYP-D3(BJ)/def2-SVP). Contour line diagrams of the Laplacian distribution $\nabla^2\rho(r)$ in the PHC ring plane. Dashed red lines indicate areas of charge concentration ($\nabla^2\rho(r)<0$) while solid blue lines show areas of charge depletion ($\nabla^2\rho(r)>0$). The thick solid lines connecting the atomic nuclei are the bond paths and the small dots are the critical points. Bond Critical Points (in black), Ring Critical Points (in red).

**Table S7. EDA-NOCV results (in kcal/mol) on the $C_{carb}$-B bond of 4a/b and 7b at the BP86-D3(BJ)/TZ2P level of theory.[a]**

| | 4a | 4b | 7b |
|---|---|---|---|
| $\Delta E_{int}$ | -72.1 | -70.7 | -68.4 |
| $\Delta E_{Pauli}$ | 179.5 | 177.6 | 192.1 |
| $\Delta E_{disp}$[b] | -4.6 (1.8 %) | -4.8 (1.9 %) | -14.7 (5.6 %) |
| $\Delta E_{elstat}$[b] | -133.7 (53.1 %) | -130.7 (52.7 %) | -126.2 (48.4 %) |
| $\Delta E_{orb}$[b] | -113.3 (45.0 %) | -112.8 (45.4 %) | -119.7 (45.9 %) |
| $\Delta E_{orb\text{-}\sigma}$[c] | -92.7 (81.8 %) | -92.3 (81.8 %) | -93.3 (77.9 %) |
| $\Delta E_{orb\text{-}\pi}$[c] | -6.1 (5.4 %) | -6.1 (5.4 %) | -7.8 (6.5 %) |
| $\Delta E_{orb\text{-}rest}$[c] | -14.5 (12.9 %) | -14.5 (12.8 %) | -18.6 (15.6 %) |
| $\Delta E_{prep\ BR3}$ | 31.2 | 30.9 | 26.4 |
| $\Delta E_{prep\ PHC}$ | 2.5 | 2.3 | 2.0 |
| $\Delta E_{prep\ total}$ | 33.7 | 33.2 | 28.4 |
| $D_e$ | 38.4 | 37.5 | 40.0 |

[a] Geometries optimized at the B3LYP-D3(BJ)/def2-SVP level of theory. [b] The value in parenthesis gives the percentage contribution to the total attractive interactions $\Delta E_{elstat} + \Delta E_{orb} + \Delta E_{disp}$. [c] The values in parenthesis gives the percentage contribution to the total orbital interaction.

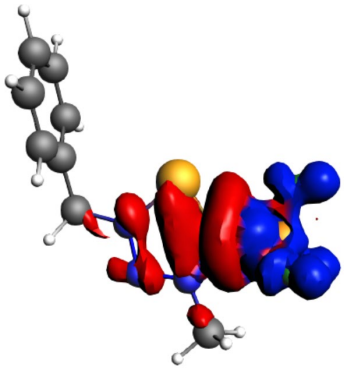

$\Delta E_{orb\text{-}\sigma}$= -92.7; |ν|= 0.72

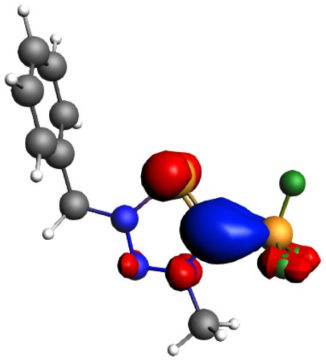

$\Delta E_{orb\text{-}\pi}$= -6.11; |ν|= 0.21

**4a**

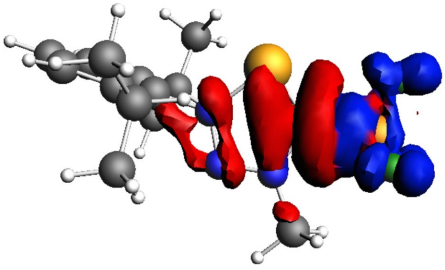

$\Delta E_{orb\text{-}\sigma}$= -92.3 kcal/mol; |ν|= 0.73

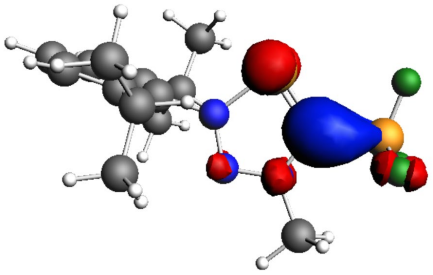

$\Delta E_{orb\text{-}\pi}$= -6.1 kcal/mol; |ν|= 0.21

**4b**

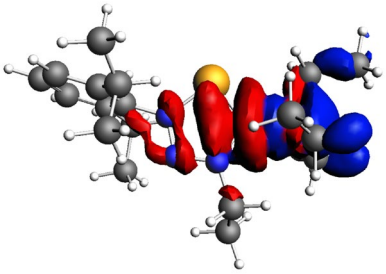

$\Delta E_{orb\text{-}\sigma}$ = -93.3 kcal/mol; |ν|= 0.74

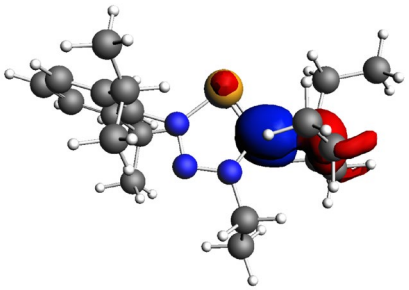

$\Delta E_{orb\text{-}\pi}$ = -7.8 kcal/mol; |ν|= 0.36

**7b**

**Figure S45.** Plot of deformation densities Δρ of the pairwise orbital interactions (isovalue 0.001 au), associated energies ΔE in kcal/mol and eigenvalues ν in a.u.. The red color shows the charge outflow, whereas blue shows charge density accumulation.

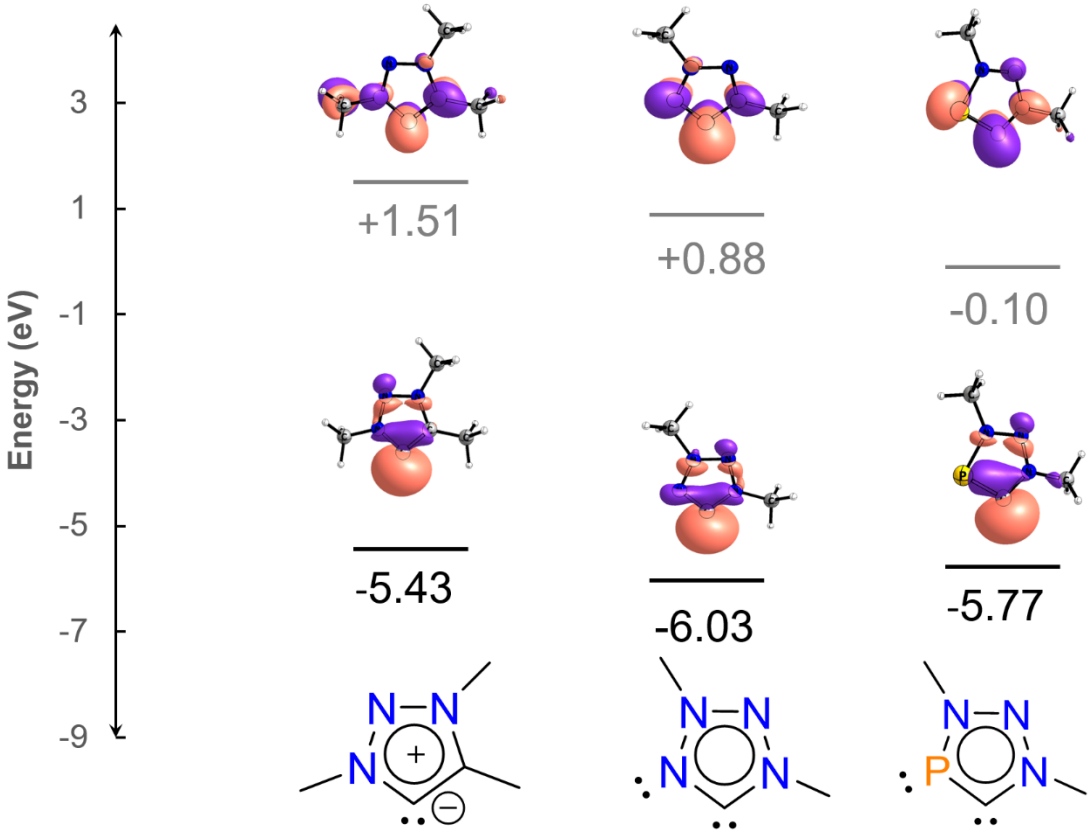


**Figure S46**. Molecular orbital energies (in eV) for the lone pairs (σ) and the unoccupied π* orbitals of 1,2,3-triazolylidene, tetrazol-5-ylidene and triazaphosphole-5-ylidene models systems at the B3LYP-D3(BJ)/def2-TZVPP// B3LYP-D3(BJ)/def2-SVP level of theory.

## 5.1 Computational Details

Geometry optimizations were performed using the Gaussian 16 optimizer[10] together with TurboMole V7.0.[11] energies and gradients. All geometry optimizations were computed using the functional B3LYP[12,13] functional with Grimme dispersion corrections D3[14] and the Becke-Jonson damping function[15] in combination with the def2-SVP basis set.[16] The stationary points were located with the Berny algorithm[17] using redundant internal coordinates. Analytical Hessians were computed to determine the nature of stationary points (one and zero imaginary frequencies for transition states and minima, respectively)[18] and to calculate unscaled zero-point energies (ZPEs) as well as thermal corrections and entropy effects using the standard statistical-mechanics relationships for an ideal gas

The atomic partial charges were estimated with the natural bond orbital (NBO)[19,20] method using NBO 7.0.[21] The topological quantum theory of atoms in molecules (QTAIM),[22] and Laplacian of the electron density analyses were carried out with AIMAII.[23] All these analysis were performed at the B3LYP-D3(BJ)/def2-TZVPP level of theory.

The nature of the chemical bonds were investigated by means of the Energy Decomposition Analysis (EDA) method, which was developed by Morokuma[24] and by Ziegler and Rauk.[25,26] The bonding analysis focuses on the instantaneous interaction energy $\Delta E_{\text{int}}$ of a bond A–B between two fragments A and B in the particular electronic reference state and in the frozen geometry AB. This energy is divided into four main components (Eq S1).

$$\Delta E_{\text{int}} = \Delta E_{elst} + \Delta E_{Pauli} + \Delta E_{orb} + \Delta E_{disp} \qquad \text{(S1)}$$

The term $\Delta E_{elst}$ corresponds to the quasiclassical electrostatic interaction between the unperturbed charge distributions of the prepared atoms (or fragments) and it is usually attractive. The Pauli repulsion $\Delta E_{Pauli}$ is the energy change associated with the transformation from the superposition of the unperturbed wave functions (Slater determinant of the Kohn-Sham orbitals) of the isolated fragments to the wave function $\Psi_0 = N\hat{A}[\Psi^A\Psi^B]$, which properly obeys the Pauli principle through explicit antisymmetrization ($\hat{A}$ operator) and renormalization (N = constant) of the product wave function. It comprises the destabilizing interactions between electrons of the same spin on either fragment. The orbital interaction $\Delta E_{orb}$ accounts for charge transfer and polarization effects.[27] In the case that the Grimme dispersion corrections[14,15] are computed the term $\Delta E_{disp}$ is added to equation S1. Further details on the EDA method can be found in the literature.[28,29] In the case of the dimers, relaxation of the fragments to their equilibrium geometries at the electronic ground state is termed $\Delta E_{prep}$, because it may be considered as preparation energy for chemical bonding. The addition of $\Delta E_{prep}$ to the intrinsic interaction energy $\Delta E_{int}$ gives the total energy $\Delta E$, which is, by definition, the opposite sign of the bond dissociation energy $D_e$:

$$\Delta E(-D_e) = \Delta E_{\text{int}} + \Delta E_{prep} \quad \text{(S2)}$$

The EDA–NOCV method combines the EDA with the natural orbitals for chemical valence (NOCV) to decompose the orbital interaction term $\Delta E_{orb}$ into pairwise contributions. The NOCVs $\Psi_i$ are defined as the eigenvector of the valence operator, $\hat{V}$, given by Equation (S3).

$$\hat{V}\Psi_i = v_i\Psi_i \quad \text{(S3)}$$

In the EDA–NOCV scheme the orbital interaction term, $\Delta E_{orb}$, is given by Equation (S4),

$$\Delta \mathrm{E}_{\mathrm{orb}} = \sum_{\mathrm{k}} \Delta \mathrm{E}_{\mathrm{k}} = \sum_{\mathrm{k}=1}^{\mathrm{N}/2} v_k \left[ -\mathrm{F}_{-\mathrm{k},\mathrm{k}}^{\mathrm{TS}} + \mathrm{F}_{\mathrm{k},\mathrm{k}}^{\mathrm{TS}} \right] \quad \text{(S4)}$$

in which $\mathrm{F}_{-\mathrm{k},-\mathrm{k}}^{\mathrm{TS}}$ and $\mathrm{F}_{\mathrm{k},\mathrm{k}}^{\mathrm{TS}}$ are diagonal transition state Kohn–Sham matrix elements corresponding to NOCVs with the eigenvalues $-v_k$ and $v_k$, respectively. The $\Delta E_k^{orb}$ term for a particular type of bond is assigned by visual inspection of the shape of the deformation density $\Delta\rho_k$. The latter term is a measure of the size of the charge deformation and it provides a visual notion of the charge flow that is associated with the pairwise orbital interaction. The EDA–NOCV scheme thus provides both qualitative and quantitative information about the strength of orbital interactions in chemical bonds. The EDA-NOCV calculations were carried out with ADF2019.101. The basis sets for all elements have triple-ζ quality augmented by two sets of polarizations functions and one set of diffuse function. Core electrons were treated by the frozen-core approximation. This level of theory is denoted BP86-D3(BJ)/TZ2P.[30] Scalar relativistic effects have been incorporated by applying the zeroth-order regular approximation (ZORA).[31]

**xyz coordinations (in Å) and Energies (in Hartree)**

**4a**

**Energy(B3LYP-D3(BJ)/def2-SVP) = -1178.45912782**

| | | | |
|---|---|---|---|
| P | -0.134390000000 | -0.597706000000 | -0.335633000000 |
| F | -3.999540000000 | -0.638180000000 | -0.974486000000 |
| F | -2.700853000000 | -2.377127000000 | -0.169975000000 |
| F | -3.675381000000 | -0.869798000000 | 1.291273000000 |
| N | 0.274992000000 | 1.104867000000 | -0.221616000000 |
| N | -0.705072000000 | 1.932281000000 | -0.005514000000 |
| N | -1.822008000000 | 1.241000000000 | 0.074921000000 |
| C | -1.763697000000 | -0.106995000000 | -0.071349000000 |
| C | 1.616458000000 | 1.704333000000 | -0.390630000000 |
| H | 1.669578000000 | 2.554364000000 | 0.303543000000 |
| H | 1.682231000000 | 2.096836000000 | -1.416476000000 |
| C | 2.703664000000 | 0.696465000000 | -0.128818000000 |
| C | 3.351393000000 | 0.056226000000 | -1.192971000000 |
| H | 3.086340000000 | 0.314265000000 | -2.221681000000 |
| C | 4.328144000000 | -0.911713000000 | -0.946334000000 |
| H | 4.827036000000 | -1.406166000000 | -1.782650000000 |
| C | 4.661727000000 | -1.247246000000 | 0.367764000000 |
| H | 5.423653000000 | -2.005550000000 | 0.561812000000 |
| C | 4.020137000000 | -0.611283000000 | 1.435826000000 |
| H | 4.280622000000 | -0.870648000000 | 2.464315000000 |
| C | 3.046653000000 | 0.356372000000 | 1.188363000000 |
| H | 2.542757000000 | 0.849862000000 | 2.023829000000 |
| C | -3.070052000000 | 1.968849000000 | 0.330932000000 |
| H | -3.500945000000 | 1.589890000000 | 1.265681000000 |
| H | -3.767570000000 | 1.742359000000 | -0.484519000000 |
| H | -2.838425000000 | 3.037285000000 | 0.389141000000 |
| B | -3.121883000000 | -1.069609000000 | 0.023794000000 |

**4b**

**Energy(B3LYP-D3(BJ)/def2-SVP) = -1374.92121233**

| | | | |
|---|---|---|---|
| P | -0.965251000000 | 0.168110000000 | -1.298646000000 |
| F | -4.408914000000 | 1.123071000000 | 0.290598000000 |
| F | -4.409253000000 | -1.158865000000 | -0.003934000000 |
| F | -4.050405000000 | 0.235230000000 | -1.816767000000 |
| N | 0.122973000000 | -0.009627000000 | 0.064635000000 |
| N | -0.428456000000 | -0.162029000000 | 1.237380000000 |
| N | -1.734580000000 | -0.142147000000 | 1.085987000000 |
| C | -2.247378000000 | 0.020539000000 | -0.162029000000 |
| C | 1.566495000000 | -0.004477000000 | -0.006998000000 |
| C | 2.230598000000 | -1.238715000000 | -0.149887000000 |
| C | 3.626752000000 | -1.201493000000 | -0.250180000000 |
| H | 4.182287000000 | -2.133763000000 | -0.358684000000 |
| C | 4.317116000000 | 0.010239000000 | -0.214160000000 |
| H | 5.406328000000 | 0.015829000000 | -0.298347000000 |
| C | 3.627932000000 | 1.212793000000 | -0.070622000000 |
| H | 4.182249000000 | 2.152451000000 | -0.043122000000 |
| C | 2.230980000000 | 1.234226000000 | 0.040435000000 |

| | | | |
|---|---|---|---|
| C | 1.472570000000 | -2.557859000000 | -0.134846000000 |
| H | 0.442438000000 | -2.354843000000 | -0.466521000000 |
| C | 1.394221000000 | -3.106750000000 | 1.301044000000 |
| H | 0.805440000000 | -4.037348000000 | 1.328102000000 |
| H | 0.925684000000 | -2.379645000000 | 1.980206000000 |
| H | 2.402730000000 | -3.328595000000 | 1.685896000000 |
| C | 2.053897000000 | -3.599375000000 | -1.097763000000 |
| H | 3.046569000000 | -3.949981000000 | -0.774024000000 |
| H | 2.150074000000 | -3.197560000000 | -2.117974000000 |
| H | 1.396587000000 | -4.481364000000 | -1.138183000000 |
| C | 1.481852000000 | 2.551966000000 | 0.173302000000 |
| H | 0.447373000000 | 2.325670000000 | 0.469722000000 |
| C | 2.072702000000 | 3.448642000000 | 1.269764000000 |
| H | 2.122272000000 | 2.920756000000 | 2.234316000000 |
| H | 1.449348000000 | 4.346674000000 | 1.401039000000 |
| H | 3.088964000000 | 3.789634000000 | 1.016930000000 |
| C | 1.424157000000 | 3.278830000000 | -1.180254000000 |
| H | 0.948860000000 | 2.653212000000 | -1.951240000000 |
| H | 2.436328000000 | 3.534942000000 | -1.532481000000 |
| H | 0.845767000000 | 4.212108000000 | -1.095040000000 |
| C | -2.570961000000 | -0.298523000000 | 2.281840000000 |
| H | -3.201053000000 | -1.185406000000 | 2.142856000000 |
| H | -3.224955000000 | 0.578769000000 | 2.355069000000 |
| H | -1.912074000000 | -0.394308000000 | 3.150845000000 |
| B | -3.890091000000 | 0.058512000000 | -0.450526000000 |

**7b**

**Energy(B3LYP-D3(BJ)/def2-SVP) = -1352.27572773**

| | | | |
|---|---|---|---|
| P | -0.454750000000 | -0.191518000000 | -1.258740000000 |
| N | 0.750923000000 | -0.015716000000 | -0.002866000000 |
| N | 0.308706000000 | 0.131643000000 | 1.212108000000 |
| N | -1.009533000000 | 0.108491000000 | 1.187207000000 |
| C | -1.653695000000 | -0.056972000000 | -0.008884000000 |
| C | 2.181023000000 | -0.032863000000 | -0.200565000000 |
| C | 2.842481000000 | -1.275455000000 | -0.171374000000 |
| C | 4.226985000000 | -1.264014000000 | -0.384918000000 |
| H | 4.780987000000 | -2.203320000000 | -0.368802000000 |
| C | 4.906783000000 | -0.068679000000 | -0.617144000000 |
| H | 5.986592000000 | -0.083162000000 | -0.782900000000 |
| C | 4.219953000000 | 1.144644000000 | -0.640569000000 |
| H | 4.768052000000 | 2.069971000000 | -0.822375000000 |
| C | 2.835199000000 | 1.191496000000 | -0.433561000000 |
| C | 2.096693000000 | -2.563372000000 | 0.146709000000 |
| H | 1.049775000000 | -2.428333000000 | -0.165733000000 |
| C | 2.093025000000 | -2.810082000000 | 1.666171000000 |
| H | 1.658887000000 | -1.956424000000 | 2.206876000000 |
| H | 3.120185000000 | -2.958791000000 | 2.037056000000 |
| H | 1.506483000000 | -3.710039000000 | 1.910262000000 |
| C | 2.635559000000 | -3.780487000000 | -0.612472000000 |
| H | 2.678695000000 | -3.594044000000 | -1.696449000000 |
| H | 1.981361000000 | -4.648996000000 | -0.441035000000 |
| H | 3.644960000000 | -4.063586000000 | -0.274101000000 |
| C | 2.081225000000 | 2.512603000000 | -0.394216000000 |
| H | 1.030486000000 | 2.303508000000 | -0.647762000000 |
| C | 2.104153000000 | 3.090197000000 | 1.032402000000 |
| H | 1.508853000000 | 4.015640000000 | 1.085989000000 |

| | | | |
|---|---|---|---|
| H | 3.136042000000 | 3.328407000000 | 1.337413000000 |
| H | 1.695448000000 | 2.371475000000 | 1.757452000000 |
| C | 2.593239000000 | 3.533337000000 | -1.416295000000 |
| H | 2.614830000000 | 3.110915000000 | -2.432492000000 |
| H | 3.607372000000 | 3.887377000000 | -1.172203000000 |
| H | 1.936051000000 | 4.416422000000 | -1.427121000000 |
| C | -1.659422000000 | 0.320232000000 | 2.494057000000 |
| H | -1.119322000000 | -0.305629000000 | 3.217639000000 |
| H | -2.679052000000 | -0.059852000000 | 2.391322000000 |
| C | -1.638220000000 | 1.786850000000 | 2.900477000000 |
| H | -2.165529000000 | 2.404392000000 | 2.160185000000 |
| H | -0.606217000000 | 2.155034000000 | 3.001424000000 |
| H | -2.144512000000 | 1.906248000000 | 3.870131000000 |
| C | -4.058317000000 | 1.152202000000 | 0.226871000000 |
| H | -5.130991000000 | 0.994137000000 | 0.011815000000 |
| H | -4.019171000000 | 1.260671000000 | 1.326952000000 |
| C | -3.610324000000 | 2.465109000000 | -0.422477000000 |
| H | -3.725260000000 | 2.430086000000 | -1.518190000000 |
| H | -2.540581000000 | 2.671228000000 | -0.233007000000 |
| H | -4.176003000000 | 3.343812000000 | -0.065257000000 |
| C | -3.412975000000 | -0.419563000000 | -1.907243000000 |
| H | -2.887369000000 | 0.390740000000 | -2.455098000000 |
| H | -2.895022000000 | -1.350902000000 | -2.216218000000 |
| C | -4.850530000000 | -0.479505000000 | -2.432119000000 |
| H | -5.389861000000 | 0.461787000000 | -2.236099000000 |
| H | -5.424833000000 | -1.282371000000 | -1.940922000000 |
| H | -4.901500000000 | -0.662889000000 | -3.519553000000 |
| C | -3.811531000000 | -1.534923000000 | 0.544447000000 |
| H | -3.967240000000 | -1.319846000000 | 1.619748000000 |
| H | -4.829335000000 | -1.735600000000 | 0.163645000000 |
| C | -2.972020000000 | -2.809670000000 | 0.412116000000 |
| H | -2.794020000000 | -3.065751000000 | -0.646090000000 |
| H | -3.442272000000 | -3.690464000000 | 0.883253000000 |
| H | -1.975437000000 | -2.695045000000 | 0.877326000000 |
| B | -3.263332000000 | -0.202296000000 | -0.275921000000 |

## 6. Literature


[1] C. Pardin, I. Roy, W. D. Lubell, J. W. Keillor, *Chem. Biol. Drug Des.* **2008**, *72*, 189–196.

[2] G. Guisado-Barrios, J. Bouffard, B. Donnadieu, G. Bertrand, *Angew. Chem. Int. Ed*. **2010**, *49*, 4759–4762.

[3] C. E. Averre, M. P. Coles, I. R. Crossley, I. J. Day, *Dalton Trans*. **2012**, *41*, 278–284; S. M. Mansell, M. Green, R. J. Kilby, M. Murray, C. A. Russell, *C. R. Chim*. **2010**, *13*, 1073–1081.

[4] J. A. W. Sklorz, S. Hoof, N. Rades, N. De Rycke, L. Könczöl, D. Szieberth, M. Weber, J. Wiecko, L. Nyulászi, M. Hissler, C. Müller, *Chem. Eur.J.* **2015**, *21*, 11096–11109.

[5] Bruker (2010). APEX2, SAINT, SADABS and XSHELL. Bruker AXS Inc., Madison, Wisconsin, USA.

[6] G. M. Sheldrick, *Acta Cryst*. **2015**, C71, 3;

[7] G. M. Sheldrick, *Acta Cryst*. **2015,** A71, 3.

[8] Spek, A. L. *Acta Cryst.* **2009**, D65 (2), 148.

[9] O. V. Dolomanov, L. J. Bourhis, R. J Gildea, J. A. K. Howard, H. Puschmann, *J. Appl. Cryst.* **2009**, *42*, 339

[10] M. J. Frisch; G. W. Trucks; H. B. Schlegel; G. E. Scuseria; M. A. Robb; J. R. Cheeseman; G. Scalmani; V. Barone; B. Mennucci; G. A. Petersson; H. Nakatsuji; M. Caricato; X. Li; H. P. Hratchian; A. F. Izmaylov; J. Bloino; G. Zheng; J. L. Sonnenberg; M. Hada; M. Ehara; K. Toyota; R. Fukuda; J. Hasegawa; M. Ishida; T. Nakajima; Y. Honda; O. Kitao; H. Nakai; T. Vreven; J. A. Montgomery, J.; J. E. Peralta; F. Ogliaro; M. Bearpark; J. J. Heyd; E. Brothers; K. N. Kudin; V. N. Staroverov; R. Kobayashi; J. Normand; K. Raghavachari; A. Rendell; J. C. Burant; S. S. Iyengar; J. Tomasi; M. Cossi; N. Rega; J. M. Millam; M. Klene; J. E. Knox; J. B. Cross; V. Bakken; C. Adamo; J. Jaramillo; R. Gomperts; R. E. Stratmann; O. Yazyev; A. J. Austin; R. Cammi; C. Pomelli; J. W. Ochterski; R. L. Martin; K. Morokuma; V. G. Zakrzewski; G. A. Voth; P. Salvador; J. J. Dannenberg; S. Dapprich; A. D. Daniels; O. Farkas; J. B. Foresman; J. V. Ortiz; J. Cioslowski; D. J. Fox Gaussian 09, Revision C.01. Gaussian, Inc.: Wallingford CT, 2009.

[11] TURBOMOLE V7.0 2015 a development of University of Karlsruhe and Forschungszentrum Karlsruhe GmbH, 1989-2007; TURBOMOLE GmbH, since 2007; available from http://www.turbomole.com: Karlsruhe.

[12] Becke, A. D., Density-functional thermochemistry. III. The role of exact exchange. *J. Chem. Phys.* **1993**, 98 (7), 5648-5652.

[13] Lee, C.; Yang, W.; Parr, R. G., Development of the Colle-Salvetti correlation-energy formula into a functional of the electron density. *Phys. Rev. B* **1988**, *37* (2), 785-789.

[14] Grimme, S.; Antony, J.; Ehrlich, S.; Krieg, H., A consistent and accurate ab initio parametrization of density functional dispersion correction (DFT-D) for the 94 elements H-Pu. *J. Chem. Phys*. **2010**, 132 (15).

[15] Grimme, S.; Ehrlich, S.; Goerigk, L., Effect of the Damping Function in Dispersion Corrected Density Functional Theory. *J. Comp. Chem.* **2011,** *32* (7), 1456-1465.

[16] Weigend, F.; Ahlrichs, R., Balanced basis sets of split valence, triple zeta valence and quadruple zeta valence quality for H to Rn: Design and assessment of accuracy. *Phys. Chem. Chem. Phys.* **2005**, *7* (18), 3297-3305.

[17] Peng, C. Y.; Ayala, P. Y.; Schlegel, H. B.; Frisch, M. J., Using redundant internal coordinates to optimize equilibrium geometries and transition states. *J. Comp. Chem*. **1996,** *17* (1), 49-56.

[18] McIver, J. W.; Komornic.A, Structure of Transition-state in organic reactions - General theory and an applications to cyclobutene-butadiene isomerization using a semiempirical molecular-orbital method. *J. Am. Chem. Soc*. **1972,** *94* (8), 2625-2633.

[19] Reed, A. E.; Weinstock, R. B.; Weinhold, F., Natural-population analysis. *J. Chem. Phys.* **1985**, *83* (2), 735-746.

[20] Reed, A. E.; Curtiss, L. A.; Weinhold, F., Intermolecular interactions from a natural bond orbital, donor-acceptor viewpoint. *Chem. Rev.* **1988**, *88* (6), 899-926.

[21] Glendening, E. D.; Landis, C. R.; Weinhold, F., NBO 7.0: New Vistas in Localized and Delocalized Chemical Bonding Theory. *J. Comp. Chem.* **2019**, *40* (25), 2234-2241.
[22] Bader, R. F. W., Atoms in Molecules: A Quantum Theory, Clarendon, Oxford, 1990.
[23] Keith, T. A.; Gristmill, T. K. AIMAll, 19.02.13; Overland Park KS, USA (aim.tkgristmill.com), 2019.
[24] Morokuma, K., Moluecular orbital studies of hydrogen bonds 3. C=O H-O hydrogen bond in H2CO and H2O and H2CO 2H2O. J. Chem. Phys. 1971, 55 (3), 1236-1244.
[25] Ziegler, T.; Rauk, A., Theoretical-study of the ethylene-metal bond in complexes between Cu+, Ag+, Au+, Pt0, or Pt2+ and ethylene, based on the Hartree-Fock Slater Transition-State method. *Inorg. Chem.* **1979,** 18 (6), 1558-1565.
[26] Ziegler, T.; Rauk, A., CO, CS, N2, PF3, and CNCH3 as s-donors and p-acceptors - Theoretical-study by the Hartree-Fock-Slater Transition-State method. *Inorg. Chem.* **1979,** *18* (7), 1755-1759.
[27] Bickelhaupt, F. M.; Nibbering, N. M. M.; Van Wezenbeek, E. M.; Baerends, E. J., *J. Phys. Chem.* **1992**, 96 (12), 4864-4873.
[28] Bickelhaupt, F. M.; Baerends, E. J., Kohn-Sham density functional theory: Predicting and understanding chemistry. In Reviews in Computational Chemistry, Lipkowitz, K. B.; Boyd, D. B., Eds. 2000; Vol. 15, pp 1-86.
[29] te Velde, G.; Bickelhaupt, F. M.; Baerends, E. J.; Fonseca Guerra, C.; van Gisbergen, S. J. A.; Snijders, J. G.; Ziegler, T., Chemistry with ADF. *J. Comp. Chem*. **2001,** 22 (9), 931-967.
[30] Krijn, J.; Baerends, E. J., Fit Functions in the HFS-Method 1984.
[31] Van Lenthe, E.; Baerends, E. J.; Snijders, J. G., Relativistic regular two-component Hamiltonians. *J. Chem. Phys*. **1993,** *99* (6), 4597-4610.[]